LBL-11981
UC-70

Lawrence Berkeley Laboratory
UNIVERSITY OF CALIFORNIA, BERKELEY

EARTH SCIENCES DIVISION

A MONITOR FOR DETECTING NUCLEAR-WASTE LEAKAGE IN A SUBSURFACE REPOSITORY

S. Klainer, T. Hirschfeld, H. Bowman, F. Milanovich,
D. Perry, and D. Johnson

November 1980

Prepared for the U.S. Department of Energy under Contract W-7405-ENG-48

TABLE OF CONTENTS

LIST OF FIGURES

EXECUTIVE SUMMARY

PROGRESS IN REMOTE FIBER FLUORIMETRY

A remote fiber optics system will be employed in conjunction with the coprecipitation enhanced fluorimetry technique. The purpose of this part of the program is to demonstrate an in situ monitoring capability using fiber optics to "effect communication" between the instrumentation and the sample. In this case the sample will be an actinide or a tracer material leacking from an underground nuclear waste repository into the ground water. A lanthanide (which are excellent fluorescent agents), actinide or other species which does not radiation damage can be chosen as the tracer to maximize sensitivity specificity and relevance. Pending arrival of the desired inorganic taggants for testing the remote fiber fluorimeter, tests were done on a number of synthetic dye taggants with the results shown in Table I.

The use of a variety of taggants having variable excitation and emission wavelengths created a need for an acromatic retroreflective fiber coupler. This was done using the geometrical properties of the fiber to design a coupler requiring no dichroics or glossy energy-splitting surfaces. Fig. i shows this system graphically. It is under construction now that the necessary components have been received.

To test the concept of reactive layer coated optrodes, a plain termination sensor was coated with a rubrene-polystyrene gel to make a selective iodine sensor via the quenching of rubrene fluorescence by iodine partitioning into the organic phase, as seen in Fig. ii. Fig. iii shows the resulting data when the optrode was immersed in an I_2-containing solution.

A detailed numerical analysis of effective pathlength in remote fiber fluorimetry shows it to be proportional to the diameter. This led to the choice of a Maxwell Light QF200A fiber as an optimum compromise between a good spectral transmission function, large core diameter, and reasonable numerical aperture. These fibers have now been received and will be mounted in the system.

Table 1

Representative fluorescent dyes and the signals they generate at a concentration of 10 ppm in the fluorescence spectrometer with a 100-m optical fiber.

	Photons/s
Acridine red	88000
Rhodamine-B	380000
Rhodamine-6G	460000
Fluorescein	170000
Dichlorofluorescein	90000
Brilliant sulphoflavine	205000
Ethidium bromide	14000
3,3" diethyloxodicarbocyanine iodide	50000
Th-1-amino-4-hydroxyanthraquinone	9000

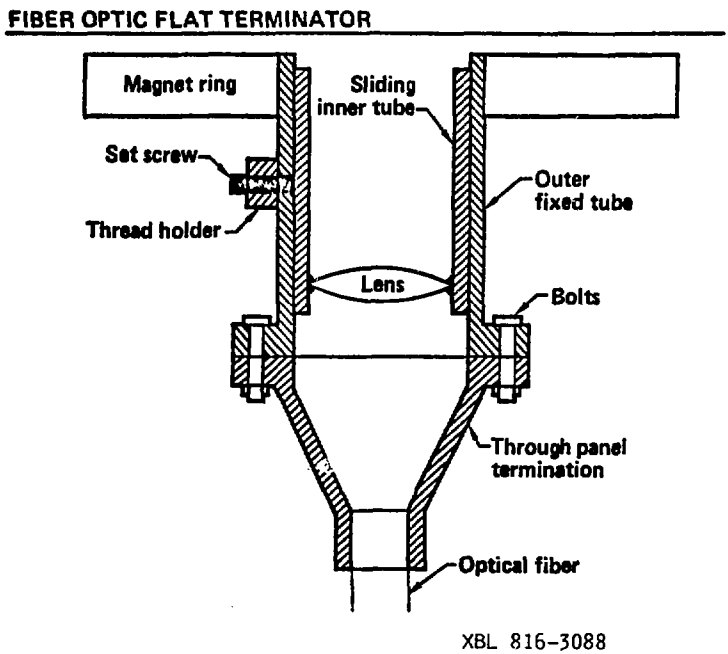

Fig. 1. Schematic for an Acromatic Retroreflective Fiber Coupler

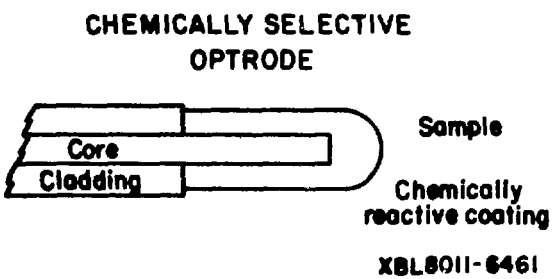

Fig. 11. Chemically Selective Optrode

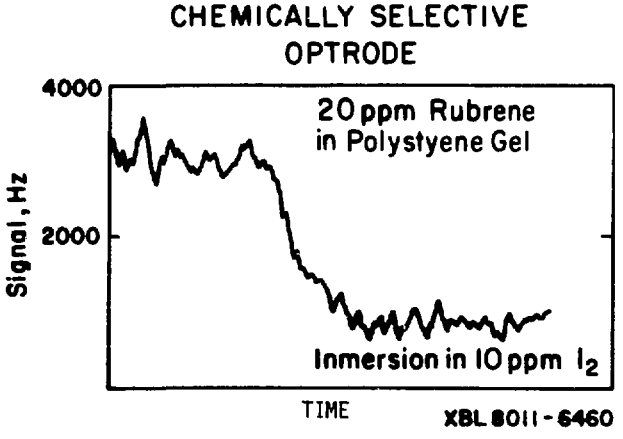

Fig. iii. Chemically Selective Optrode Used with an Iodine Solution

EXECUTIVE SUMMARY

PROGRESS IN COPRECIPITATION ENHANCED FLUORIMETRY

The ability to rapidly and conveniently determine small quantities of actinides in geomedia such as groundwater is desirable from several standpoints. With the recent emphasis on the need to have a more complete understanding of the migration of radioactive materials through soils and various types of mineral deposits (especially around nuclear waste repositories), it would be highly advantageous to have the capability of analyzing a large number of samples sensitively and rapidly. Hydrogeochemical exploration for uranium also requires routine analysis of a large number of samples for minute amounts of uranium. Finally, an accurate and precise determination of actinide trace levels in geologic surroundings is important for conducting basic geophysical research in such areas as radiometric age dating and terrestial heat-flow phenomena.

The method of analysis for the determination of actinides developed by members of the Geosciences Group at Lawrence Berkeley Laboratory and the General Chemistry Division at Lawrence Livermore National Laboratory affords a simple, cheap, easily prepared sample that can be routinely made in any laboratory using easily obtained reagents. The methodology has been evolved using the easily handled uranyl ion, UO_2^{2+}, in water solutions. It can, however, be extended to most actinides, lanthanides, and other selected ionic species. It has a routine detection limit for uranium ($<<10^{-12}$M) that far surpasses that presently demonstrated for other techniques. The analytical scheme involves a precipitation procedure and subsequent sample preparation patterned after those used by other investigators in their study of other metal ion systems such

as the lanthanides. The present techniques utilizes the ability of solution-precipitated calcium fluoride to co-precipitate uranium (in the form of the most solution stable species, the uranyl ion, UO_2^{2+}), followed by air-calcining the precipitate at elevated temperatures. The co-precipitated uranium is then spectroscopically monitored by laser-induced fluorescence excitation (LIFE). The technique has detected uranium in solution at a concentration of $<10^{-12}$ molar or 2.38×10^{-4} ppb. Its extrapolated sensitivity is 10^{-14} molar uranium. This, however, is probably not usable because of the reagent uranium background 10^{-13} M. Detection of 10^{-14} M or less plutonium is a realistic expectation. Research in this program to date, at Lawrence Berkeley Laboratory has centered on the co-precipitation of uranium in calcium fluoride matrices because uranium is an easy actinide to handle. The experimental parameters - such as calcination temperature and time, initial uranium concentration in solution, and interfering cations and anions - that affect the concomitant spectra of the samples have been investigated. Instrumentation used to obtain the spectra has also been designed, interfaced, and its performance optimized in conjunction with Lawrence Livermore National Laboratory. Detection limits, the extent of the co-precipitation of the uranium in calcium fluoride, and the selectivity of the technique have been studied, along with the application of the technique to actual uranium-containing groundwater samples. The results to date have been formally submitted for publication in Analytical Chemistry, a preprint of which is represented in Appendix I.

A Monitor for Detecting Nuclear Waste Leakage In a Subsurface Repository

I. INTRODUCTION

A new ultrasensitive analytical technique based on the laser-induced fluorescence excitation (LIFE) technique allows quantitative measurements of actinide, lathanide, and tracer abundances in water samples with sensitivities many orders of magnitude higher than presently achieved with current analytical methods. The principal focus of the present program is to develop monitoring instrumentation for those elements in ground waters associated with nuclear waste repositories. The monitoring system provides for two modes of analysis: (a) An in-situ system which provides direct remote chemical measurements in natural water systems over long distances ($\sim$1 km) using fiber optics and (b) the field laboratory system which is far more sensitive and involves (on-site) LIFE measurements on these materials after they have been coprecipitated (from ground water samples) with an inorganic material such as calcium fluoride.

Proof of principle for the remote fluorescence measurements have been made at 0.2 km using an organic fluorescent tracer and communications grade fiber optics coupled to a laboratory fluorimeter. Sensitivities in the ppb range and quantitative measurements with 1% linearity have been realized.

Initial results, using coprecipitation, have demonstrated lanthanide sensitivities of 10^{-9} ppm and uranium sensitivities below 10^{-12} ppm. It is expected that uranium will be detectable below 10^{-14} ppm when the approach is fully developed. Lanthanide sensitivities should be better.

The projected plutonium sensitivity is of the two orders of magnitude less than the uranium.

II. DESCRIPTION OF MEASUREMENT SYSTEM

A versatile laboratory fluorimeter (fluorescence spectrometer) has been assembled which is capable of making measurements utilizing both the fiber optic (remote) technique and the coprecipitation (high sensitivity) method. The spectrometer has the following components:

1. A Spectra Physics Model 171 multiline krypton laser which covers the 360 to 640 nm region with a total of 8 watts of power.
2. A Chromatix dye laser pumped by a high repetition frequency pulsed neodymium laser for continuous scanning of excitation spectra over much of the visible spectrum.
3. A Spectra Physics 165 argon laser with a total output of four watts to provide an alternate set of laser lines.
4. These lasers are then coupled, with a set of beam redirector mirrors and a Claissen filter to isolate the desired excitation wave length, to a specially made Spex right angle optical bench containing an f/1.4 illumination lens and a f/1.2 collection lens. The lenses are in alignment mounts that permit a common focus, $\sim$100μ in diameter, to be obtained in a sample holder inclined at 45°.
5. The collected light is fed at f/8 into a Spex No. 14018 750mm focal length double monochromator equipped with holographic gratings blazed at 5000 Å.
6. The monochromatized light is re-imaged at f/2 onto a cooled RCA C31034A GaAs photocathode photomultiplier (PMT) in a

6. The monochromatized light is re-imaged at f/2 onto a cooled RCA C31034A GaAs photocathode photomultiplier (PMT) in a Products for Research RF-TSA cooled housing. The PMT is operated at $\leq$ 2000 volts using a Power Design adjustable filtered HV source.
7. The photoelectron pulses are conditioned, windowed, and counted by an Ortec photon counting system consisting of an Ortec 9301 pulse discriminator, an Ortec 9302 pulse amplifer/conditioner and an Ortec 9349 ratemeter.
8. Alternatively, the signal from the discriminator is processed by a PAR model 162/164 boxcar averager to discriminate against a fast (</μs) fluorescent background.
9. The output of the ratemeter is fed to an HP 3455A electrometer having an HPIB interface and controlled by a Tektronix 184 Time Mark Generator.
10. The electrometer is in turn coupled to a Tektronix 4051 graphics processer having a flexible disk attachment, a Tektronix 4631 hardcopy generator, and a Tektronix 4662 plotter.
11. Auxiliary equipment such as laser power monitors, beam attenuators, and polarisers are also included in the system.

The performance of the system is best checked by measuring a Raman (rather than a fluorescence) spectrum. Figure 1 shows the Raman spectrum of naphthalene generated as a systems calibration check. The far lower sensitivity of the Raman phenomenon as compared to fluorescence permits the system's efficiency to be demonstrated.

III. IN-SITU MONITOR

A. Technical Approach

The in-situ monitoring of an underground waste repository is accomplished by utilizing a network of buried sensors (fiber optic devices) in and around the burial site. Specifically, a laser fluorimeter (which can be placed in a convenient location) is connected to a network of communications grade, radiation resistant, fiber optics which have sensing terminations and are buried in the repository. Here the sharp focusing abilities of the laser are used to get the light into the fiber, which carries it with remarkably little loss up to a kilometer or more to the sample. A fraction (dependent on light collection ability of fiber termination) of any fluorescence from the sample will be directed backwards toward the fiber. This will then propagate back through the fiber to the sensor. Here the returning beam is separated by a geometrical beamsplitter and measured. The concentration of naturally fluorescent compounds can be determined from the signal intensity. Nonfluorescent compounds can be determined by coating the fiber termination with appropriate extracting reagents. The sensitivity of this type of device will be below the ppb level. This would be more than adequate to detect significant container leakage, as the effluent would contain strongly fluorescent ions, such as actinides or added lanthanide tracers, in a fairly high concentration. Alternatively, the outside of the containers can be coated with fluorescent tracer ions to detect material influx (mass motion) in the immediate environment of the containers prior to any leakage occurring. As these ions are monoatomic in their stable oxidation state, they would not be radiosensitive.

Different compounds can be distinguished by choosing the excitation and observation wavelength and by choosing the coating on the fiber. Numerous locations can be monitored with one instrument by means of electroptic switchable couplers.

B. Progress During this Reporting Period

During the seven (7) months this program was active in FY80, the following was accomplished:

1. Construction of a laboratory system for routine collection and computer processing of high sensitivity, high resolution fluorescence data at ambient temperature (see Section II).
2. A fiber optic system was coupled to the laboratory spectrofluorimeter, and several fiber terminations designed.
3. Remote detection of trace concentrations of fluorescent compounds was demonstrated, and the linearity of the signal with concentration established.
4. Additional optimized parts were ordered for the fiber optics system and special mounting interfaces designed.
5. A mathematical analysis of the effective pathlength and signal levels in the fiber optic system completed.

C. Remote Fiber Fluorimetry

The possibility of remote analysis using fiber optics was first demonstrated by an instrument in which separate fibers were coupled to the laser source and to a photomultiplier and connected to a distal "optrode" in which both fibers came together at an angle. This defined a volume illuminated by the fiber coming from the laser, which lay within the field of view of the fiber going to the photomultiplier. Fluorescence arising within this volume would thus be measured by the system (see Appendix II).

Figure 2 shows the appearance of this probe, and the fluorescence it produced in a 10 part-per-million solution of the chemical rhodamine 6G, when illuminated with several milliwatts of green laser light. The sample was located outdoors at the end of a 0.2 km fiber. The signal produced by the fluorescence shown at the photomultiplier, also 0.2 km away, was several hundred thousand counts per second.

This system, however, is far from optimal. Calculations show that only a small fraction of the fluorescence from the overlap volume was collected by the fiber. An improved system, using only a single fiber, as shown in Figure 3, was then employed. This uses a beamsplitter to deliver the laser radiation returning through the fiber at a different wavelength. Here the distal end device is a simple plain termination, where the backwards-emitted fluorescence from the iluminated volume is collected by the fiber. This improved system is then coupled to a fluorescence spectrometer using lenses.

To best serve the monitoring (chemical analysis) needs, the ability of the system to perform quantitative measurements is essential. The ability of this technique to quantify was shown by testing the system with a set of solutions of different concentrations. The resulting data is shown in Figure 4. This calibration curve appears to be linear from 0.1 to 10 ppm and a detection limit of ten parts per billion could be confirmed by actual measurement. Lower detection limits should be attainable with an optimized fiber optic system. Obtaining the components to make improved systems has been very slow due to long delivery times and, often, the need for customized optics.

A mathematical derivation of the actual behavior of this fiber-optical sensor probe, or optrode (by analogy to electrode) showed its

signal level to be directly proportional to its diameter (see Appendices III and V). Since this is limited by commercial fiber availability (and eventually cost), an alternative procedure was considered which uses a lens in front of the fiber. A particularly simple version of this uses a glass (or sapphire) ball as a lens. This is accomplished by holding the fiber centered in a glass tube whose open end is then sealed with the ball. To focus the system, the fiber termination was moved along the tube axis to an optimal location before the retaining cement sets. Figure 5 shows the appearance and behavior of such a ball optrode illuminating a vial of fluorescent dye.

One of the byproducts of the fiber-optic interconnection technology, develped by the communications industry, is the ability to connect many fibers in parallel or sequentially to a single source. This provides the methodology by which a remote fiber fluorimeter can monitor a number of measurement points with a single instrument. If the range capability of these fibers is taken into account, it is easy to see how the remote fluorimeter can provide continuous and/or rapid sequential analysis of many points throughout a repository with a single instrument back at a field station where a sheltered environment exists and where data-processing equipment can be made readily available. Furthermore, the fact that the monitor is easily accessible makes it possible to easily repair, modify and upgade.

The economic advantages of a single analyzer, which can perform multipoint measurements, permit the system to be more sophisticated and versatile. Here the cost of expanding sampling locations is the relatively small one of additional fibers. The logistics of multipoint sampling, particularly when frequent observations are required, also

favor a continuous remote analyzer over the frequent, alternative choice, of a number of sample-gathering personnel traversing the system on set schedules.

Figure 6 shows the use of a typical terminal with a ball optrode in the laboratory. In practice, the fibers, and possibly tracers, would be buried with the waste and monitored from the surface. The high-radiation resistance of optical fibers is a key to the success of this approach.

Heightened sensitivity in fluorescence spectroscopy is possible by using fluorescence enhancing or producing chemical reagents. This technology will be developed for the repository monitor and can be incorporated into remote fiber fluorimetry by chemically coating the optrodes with insoluble or covalently-bound reagents. Here, of course, reversible equilibrium reactions must be chosen to avoid reagent consumption. Such a chemically specific optrode would behave much like an ion-specific electrode and be a specific detector for its target compound.

IV. High - Sensitivity Monitor

A. Technical Approach

The high-sensitivity approach is to be used to detect microleaks, for monitoring in the far field or for detecting minute contaminant levels in the groundwater. The requisite parts per trillion or less sensitivity is not available in remote detection, and it becomes necessary to recover samples for measurements within the instrument. This possible inconvenience is more than offset by an increased sensitivity of 10^2 to 10^5 orders of magnitude over extant methods. Before selecting any one approach, a very large number of techniques

were evaluated and only the coprecipitation - selective laser excitation fluorescence approach seemed sensitive enough to work at the required concentration levels.

In this technique, the sample is mixed with reagents that precipitate each other to form a host crystal lattice into which the actinide ions will coprecipitate as fluorescent species. This concentrates the actinides and separates them from background impurities and concomitant fluorescence. In this new environment, the absorption cross section of the actinide ion is enhanced and its fluorescent quantum efficiency increased. Because of the ordered nature of the crystal lattice, all the bands narrow with large increases in their peak intensity. This can be further enhanced by cooling the sample.

B. Progress During this Reporting Period

During the seven (7) months this program was active in FY80, the following was accomplished:

1. Construction of a laboratory system for routine collection and computer processing of high sensitivity, high resolution fluorescence data at ambient temperature (see Section II).
2. A literature search covering fluorescence properties of uranium and plutonium compounds and their analytical use unearthed a large number of references which were studied in detail.
3. The fluorescence behavior of uranyl-doped CaF_2 lattices at low temperature was studied using a tunable pulsed laser and time resolving electronics with the aim of better understanding the coprecipitation process.
4. An initial version of a sample preparation protocol was prepared and tested by optimizing reagent concentration and temperature.

5. Approximately 200 sample runs were undertaken to establish optimal instrument settings and determine the spectrum of uranium under a variety of operational conditions.
6. Reagent blanks for a variety of compounds were determined and sample preparation precautions were delineated to assure that background contributions were minimized.
7. The linearity of the signal with sample concentration over three orders of magnitude was established.
8. Research into the method's quantitative reproducibility was begun.
9. A minimum concentration of 10^{-12} M, several times lower than the natural uranium background concentration, was measured well above the reagent blank and noise. Calculations from this data indicate sensitivities below 10^{-14} M should be attainable.
10. Concentrations of 10^{-12} M were detected with a signal-to-noise of 50:1 using the boxcar averager. It should be noted that these measurements not make full use of the fluorimeter capability.

C. Coprecipitation Enhanced Fluorimetry

1. Preparation of Coprecipitated Samples

A $\leq$5 ml volume of 0.005M $UO_2(NO_3)_2 \cdot 6H_2O$ stock solution (slightly acidified with HNO_3 for better storage qualities) or an intermediate freshly prepared dilution (for reduced concentrations) is pipetted into an acid washed 150 ml Pyrex beaker and 5.0 ml of 1.0 M $Ca(NO_3)_2 \cdot 4H_2O$ solution added. The solution is then made up to 20 ml with triply distilled water. To this solution 30 ml of 0.3M NH_4F is added over a

55-60 second interval with continuous stirring using a Teflon coated stirring bar. After completion of the mixing, the stirring bar is removed, and the beaker is covered with Parafilm to avoid contamination.

One of the limiting problems in preparing the coprecipitated samples is reagent and water purity. Neither the best chemicals nor the most carefully distilled water meet the standards necessary for this work. At present the best materials available are suitable for measurements in the 10^{-10} M range, and these have been used for all sample preparations.

The solution is then allowed to settle for 48 hours which allows some growth of the precipitate crystals as well as the formation of a clear supernatant which can be drawn away by careful aspiration. This leaves a total volume of 5 to 10 ml. This is stirred until resuspension of the precipitate occurs, and the suspension is then transferred to a Pyrex centrifuge tube. After 15 minutes of centrifugation at moderate speed, the supernatant is drawn off and the precipitate dried, without removal from the centrifuge tube, in an oven at 105°C for 12 hours. The precipitate is then pried away from the wall of the tube and broken up with a stainless steel spatula and transferred to an agate mortar and pestle. After fine grinding, the sample is placed in a Coors crucible and calcined for three hours at a fixed temperature in a high-temperature oven. To insure reproducible calcination temperatures, the samples are always placed in fixed position within the oven. After extraction from the oven, the samples are allowed to cool and are pressed into a pellet with a non-evacuated Carver pellet press of the type used for KBr pellet preparation for infrared spectroscopy. The pellet is then placed in the fluorescence spectrometer.

The CaF_2 yield in the process is of the order of 90%, and an 80 fold concentration of the sample occurs in coprecipitation. Attempts to get higher enrichment factors by using lower Ca^{2+} and F^- concentrations led to almost colloidal precipitates which proved quite hard to separate from the solution.

The present sample preparation procedure is still excessively complex, and considerable simplification is possible by using direct filtration in a Gooch crucible instead of settling, decantation, and centrifugation. The crucible can then be calcined directly without drying. In addition, the pelletizing step can probably be eliminated by properly shaping both the filter and the sample holder in the spectrometer.

Present observations indicate that much less than 1 mm^3 of the total > 200 mm^3 sample volume contributes to the observed signal. This is limited by the practical size of the focal spot of the instrument. It should, therefore, be possible to use very small water samples, on the order of 1 m, if the appropriate microchemical and sample shaping procedures are used. Future efforts in sample preparation will center on the problems of reduced sample size and simpler preparation methods.

At present the plans are to do all the development work using uranium. In particular, all of the measurements will be made using UO_2^{2+}-containing solutions. Preliminary treatment of the sample can alter other uranium species into this form. The use of different pretreatments on successive aliquots will then allow speciation of the uranium present. Extrapolation of the co-precipitation-LIFE technique sensitivity for uranium has been calculated and shown in Appendix IV. Other modifications to be explored are the use of more concentrated

NH_4F and $Ca(NO_3)_2 \cdot 4H_2O$ solutions, accompanied by more vigorous stirring, to reduce the sample's dilution by reagent.

It should be noted that for consistency and to establish laboratory results which can be related to field measurements in the experimental work here, the UO_2^{2+} concentrations given here are those in the aqueous solution before precipitation. Furthermore, in spite of the very satisfactory behavior of CaF_2 coprecipitation, other matrices such as $ThOF_2$, $ZrOF_2$ will be explored, with the eventual intent of arriving at a single matrix suitable for both uranium and plutonium. It should be noted, however, the literature indicates that plutonium substitutes into the CaF_2 lattice as a fluorescent species as well as uranium. This is an aspect that will be explored later when final optimization of coprecipitation materials is undertaken.

2. Selective Laser Excitation of Coprecipitated Uranyl Solution Samples

Figure 7 shows a spectrum of a 10^{-5}M UO_2^{2+} sample coprecipitated in a CaF_2 matrix and calcined at 800°C. In order to keep the signal readings within the power handling capabilities of the photomultiplier tube and the ratemeter, the laser intensity had to be reduced to 5 W. As this power level is beneath the minimum laser power output, an attenuator had to be used in the laser beam. Even so, the slits had to be closed to a 3 cm^{-1} bandwidth (far smaller than required by any spectral feature) in order to keep the signal to one million counts per second. A visual examination of the sample, however, showed slight yellowing, indicating an excessive loading of the lattice with UO_2^{2+} and incipient breakdown of the crystal structure. This indicated a better performance at reduced concentration. Figure 8 shows that this

was indeed so, and 150,000 counts per second were obtained from a 10^{-7}M UO_2^{2+} sample, calcined at 550°C and measured at somewhat higher resolution. Here only 1.2 g of uranium was present of which only 6 ng was in the actual observed portion of the pellet.

It is important to note that if the entire 1200 cm^{-1} width of the band were observed by using a filter instead of scanning through the band a little at a time, as is done in the laboratory spectrometer (see Section II), 200 times larger signals could be obtained. The transmission and light gathering power increases in a filter would contribute a further ten-fold sensitivity enhancement and an additional gain factor of 400 would result from using the full laser power at the irradiation wavelength. Longer integration times of five minutes would further increase the signal 300 times. Thus an enhancement of 2.4×10^8 ($200 \cdot 10 \cdot 400 \cdot 300$) is realizable and it is possible to extrapolate a signal level of $3 \cdot 10^{13}$ counts from the low concentration of 10^{-7} m UO_2^{2+} sample. This is unrealistic. No electronic system could handle such large signals at these concentrations. Lower concentrations, compatible with the needs of an actinide monitor operating in the far field, would give more reasonable signals. The sensitivity advantage of fluorescence with its 10^3-10^6 photons/atom sample/second maximum, as compared to nuclear detection methods giving 1/2 photon/atom sample/half-life, is clearly exemplified here.

Finally, it should be pointed out that the spectra shown here were obtained before the data system was complete. In this situation, only an SSR 1105 Photon Pointer and a Gould chart recorder connected to the ratemeter analog output jack were used.

was indeed so, and 150,000 counts per second were obtained from a 10^{-7}M UO_2^{2+} sample, calcined at 550°C and measured at somewhat higher resolution. Here only 1.2 g of uranium was present of which only 6 ng was in the actual observed portion of the pellet.

Figure 9 shows the effect of varying calcination temperatures. The data, to date, indicates that 950°C gives the best results, and has consequently been used more often. In Figure 9 the size of the error bars should be noted. Deviations from reproductibility of 10% are presently observed. Present lack of reproducibility probably is due to both sample preparation inconsistencies and instrument adjustments. Improvement of the sample handling operations will be addressed first. After this, quantitative fluctuations due to spectrometer alignment and laser power fluctuations will be considered. Finally, the eventual use of internal standards or a standards addition method will be explored. Figure 10 shows an example of these optical errors on a 10^{-6} M UO_2^{2+} sample that was rerun after storing the pellet for 1 week. Figure 11 shows a system using pure reagents but no uranium. Both the background and its noise content are shown. This can be compared with Figure 12, the spectrum of a 10^{-10} M UO_2^{2+} solution, where the observed sample quantity is only 6 ng. Even without the improvements discussed previously, this amount of sample is detectable at a very substantial signal to noise ratio which is well above background. Detection limits of $< 10^{-12}$ M could probably be supported by these data, except for the natural uranium background concentration of $\sim 5 \cdot 10^{-10}$ M which is considerably above the already demonstrated measurement level.

Figure 13 shows a spectra of UO_2^+ in CaF_2 precipitated from a 10^{-12} M solution. The high signal to noise ratio (50:1) was obtained

by modulating the laser beam and signal processing via a boxcar averager. The boxcar places a variable sized window at a specified time within each modulated cycle. This allows for the detection of fluorescence during the cycle when the sample is not being illuminated. Since the uranium signal is relatively long lived, ~200 μs at room temperature, all background fluorescence with shorter lifetimes can be discriminated against using this procedure.

Figure 14 is a calibration curve relating the output voltage of the boxcar averager to the count rate the ratemeter would monitor if it could monitor only the signal received during each boxcar window. This allows these to be a comparison between spectra taken with the boxcar and spectra taken with the ratemeter.

Figure 15 shows the relative intensity of the UO_2^{2+}/CaF_2 spectra as a function of concentration. These data were obtained using the boxcar averaging system. It demonstrates the linearity of the uranyl signal strength over a concentration range of six orders of magnitude. This together with the above signal-to-noise ratio allows a reasonable extrapolation of the detection level to 10^{-14} M concentration.

An interesting observation can be made in Figures 16 and 17 which show that UO_2 and UO_3, respectively, have no or very weak fluorescence. From this data it can be seen how the CaF_2 acts not only to preconcentrate the sample and remove interferences, but how it also tremendously increases both the fluorescence efficiency and the excitation cross section of uranium compounds.

A preliminary study of contaminated water from the Femme Osage Slough gave spectra like those in Figure 18. Here a concentration of 63 ppb uranium was deduced for a sample in which neutron activation

analysis had found 70 ppb of material. For this comparatively sweet water, at least, any residual interferences do not seem too serious.

Further work on the precipitation and measurement of these samples is continuing. In its present state, it already compares very favorably with a number of other techniques for determining uranium in groundwater as seen in Table I. In fact, the 10^{-13} gms/ml with boxcar results already detected are still far from the detection limit, even without any of the planned improvements. The dramatic sensitivity of this technique is emphasized when a projected detectability of 10^{-15}g is compared to the values in the Table I. This extra sensitivity will be required when the focus becomes plutonium.

V. Summary

A. In-Situ Monitor

The remote fiber fluorimetric portion of the program is slightly ahead of schedule and proceeding well technically. Proof of principle has been demonstrated over a 0.2 km path length using an organic tracer material. Performance and design calculations have been made for the fiber optic components of the system. Optimized fibers have been ordered and special jigs and optical couplings are presently being fabricated. Future progress will be dependent on receipt of essential items.

B. High-Sensitivity Monitor

Progress on the high-sensitiivty analyzer using coprecipitation techniques has proceeded well ahead of schedule with technical results far above expectations. Preliminary measurements in the UO_2^{2+}/CaF_2 detection system has proved sensitivities well beyond the natural background limit. While further improvement of sensitivity (to 10^{-15}g) already is planned, emphasis will now be placed on locating and dealing

with possible interferences and on determining how to improve and optimize quantitative accuracy. In addition, simplication of the sample preparation procedure and downscaling to use very small (< 1 ml) groundwater samples is planned. In the longer time frame, work on maximum chemical speciation and the possibility of isotopic speciation will be undertaken. Once the coprecipitation procedures, instrumentation, and spectroscopy have been fully refined for uranium, then the process will be repeated for plutonium and perhaps americium and thorium.

Table I

•Comparison of Methods for the Determination of Uranium in Surface or Ground Water[1]

No.	Method	Enrichment or Separation	Volume (ml)	Enrichment Factor	Detection Method	Detection[2] Limit
1	Laser-induced fluorescence	direct	5	—	fluorescence	0.05ng/ml
2	Xenon arc lamp induced fluorescence	ion-exchange sulphuric acid	200	22	fluorescence	0.30ng/ml
3	Xenon lamp with Fluran	direct	5	—	fluorescence	2.00ng/ml
4	Solid fluorescence of NaF beads	extraction	5	—	fluorescence	0.50ng/ml
5	X-ray fluorescence	separation with Hyphan exchange	500	$5x10^4$	X-ray fluorescence	0.30ng/ml
6	Neutron activation	Chelex 100	1000	$5x10^3$	γ-spectroscopy	0.30ng/ml
7	Delayed neutron counting	ion-exchange suphuric acid	1000	1000	neutron counting	1.00ng/ml
8	Nuclear track method	direct	0.025	—	track counting	0.10ng/ml
9	Spectrophotometric determination (Arsenazo III)	$AlPO_4$ precipitation	500	100	absorption spectroscopy (665 nm)	2.00ng/ml
10	AAS flame	ion-exchange	1000	40	detn. of Cu	25.00ng/m/
11	AAS non-flame	ion-exchange	1000	40	detn. of Cu	2.00ng/ml
12	AAS (flame)	direct	—	—	atomic adsorp.	30.00 ppm
	Flame atomic emission	direct	—	—	atomic emiss.	10.00 ppm
	Atomic fluorescence	direct	—	—	atomic fluore.	3.00 ppm
13	Polarography	precipitation with $Fe(OH)_3$ and extraction	2000	—	polarography	2.00ng/ml
14	ICP emission spectroscopy	direct	—	—	atomic emiss.	1-10.00ng/ml
15	ICP emission spectroscopy	direct	—	—	atomic emiss.	1.50ng/ml
16	CMP emission spectroscopy	direct	—	—	atomic emiss.	30.00 ppm
17	AES carbon furnace	direct	—	—	atomic emiss.	2.50 ppm
18	Selective laser excitation[3]	coprecipitation	1	100	fluorescence	<1.00fg[4]

(1) Campen, W. and Bächmann, K., Mikrochemica Acta (Vienna), (1979) II, 159-70
(2) No background, S/N = 3:1.
(3) This work
(4) fg = 10^{-15}g

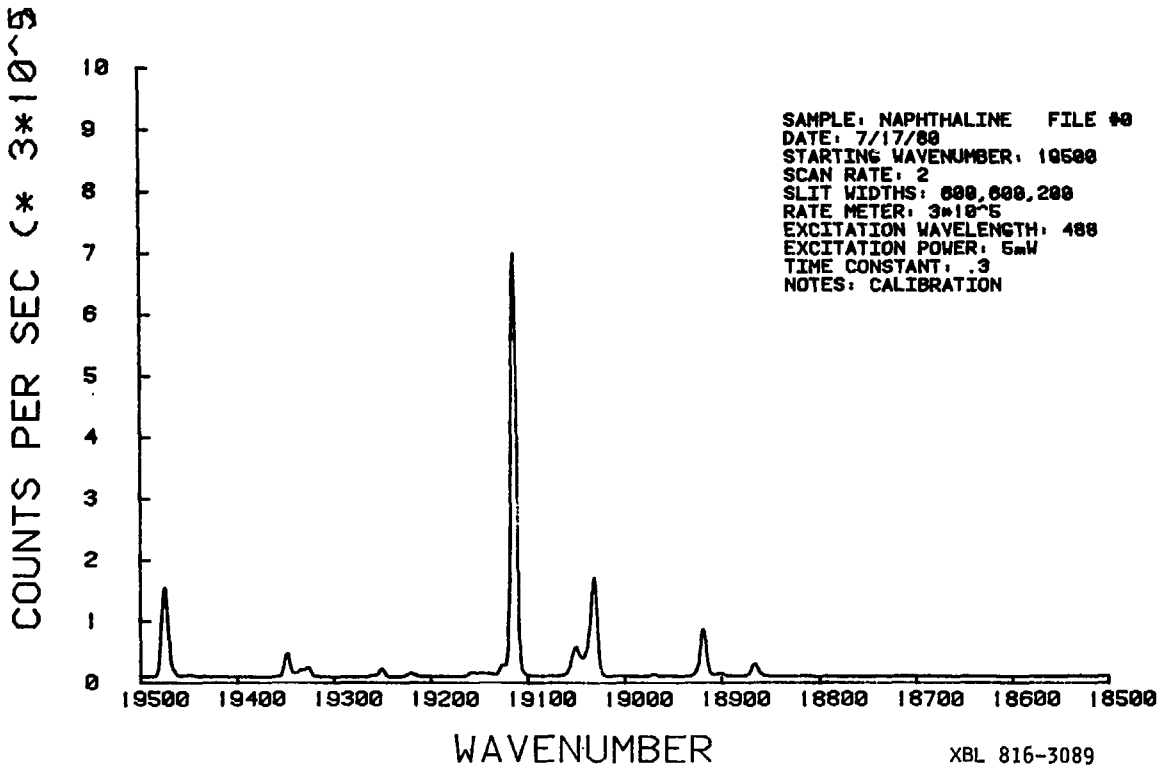

Fig. 1. Raman Spectrum of Naphthalene

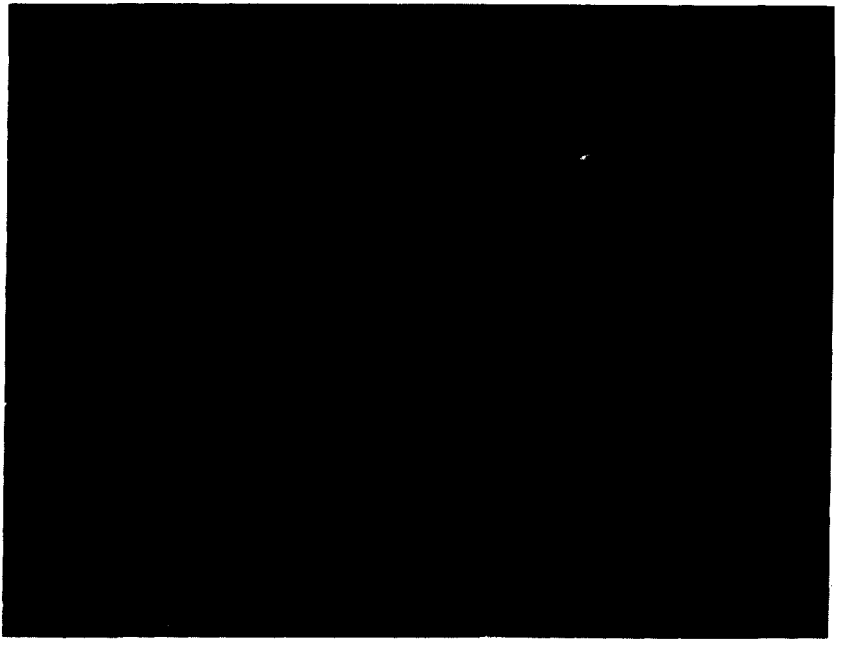

CBB 808-9292

Fig. 2. Fluorescence Excitation Using a Fiber Optic Probe

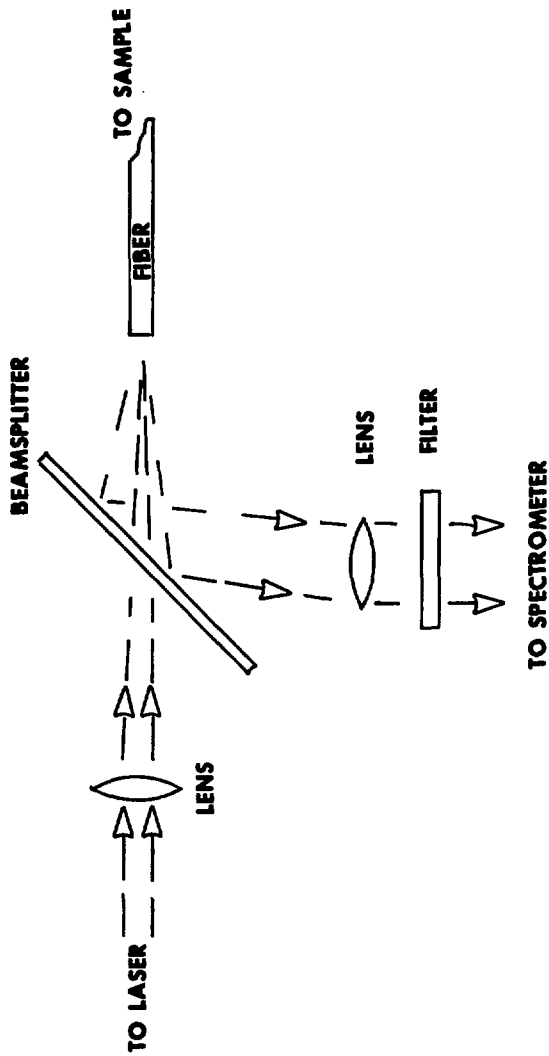

XBL 816-3090

Fig. 3. Remote Fiber Fluorimeter Beamsplitter Coupler

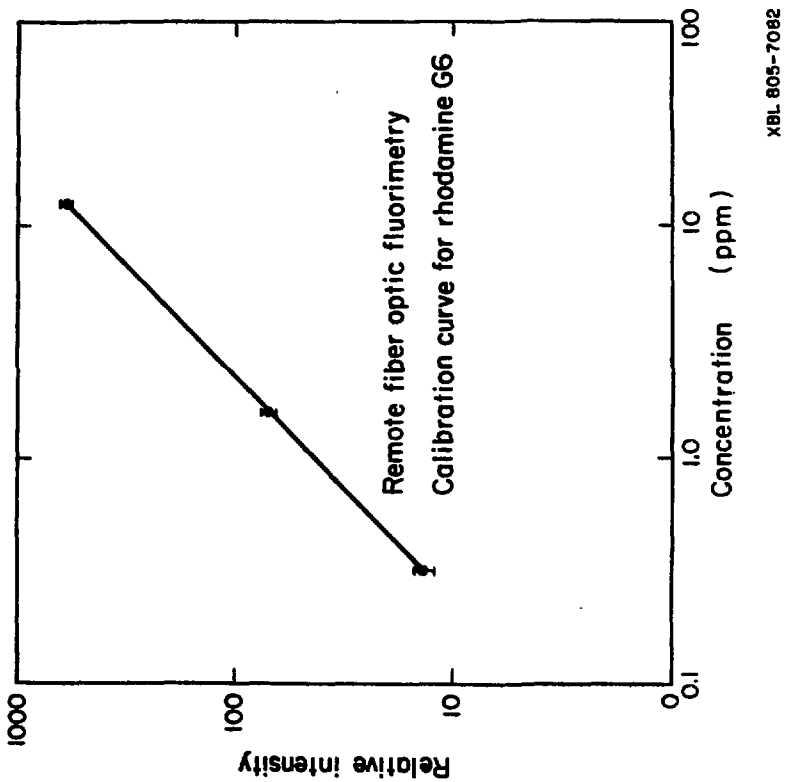

Fig. 4. Remote Fiber Optic Fluorimetry Calibration Curve for Rhodamine G6

CBB 808-9294

Fig. 5. Fluorescence Excitation Using a Ball Optrode

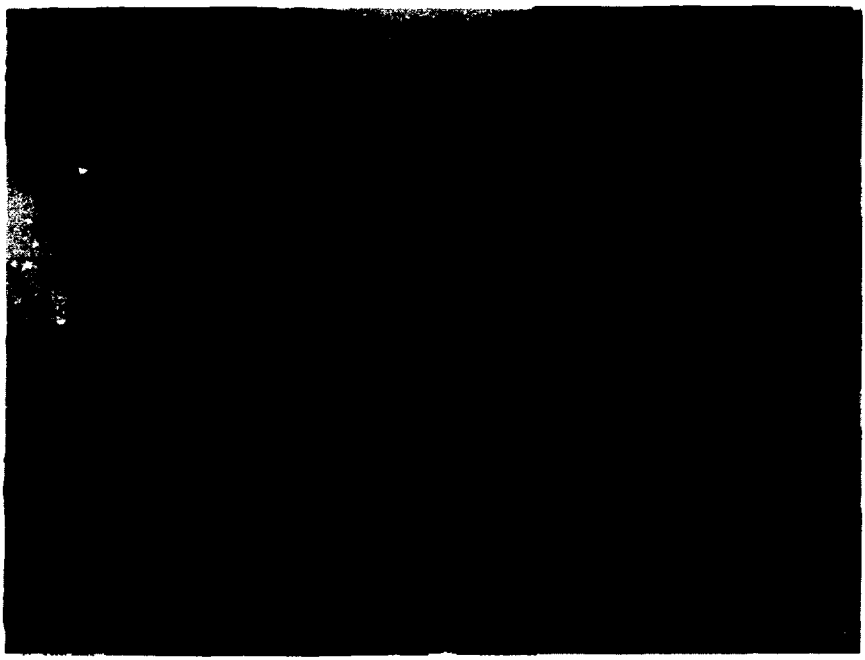

CBB 805 6056

Fig. 6. A Laboratory Fluorescence Measurement Using the Ball Optrode

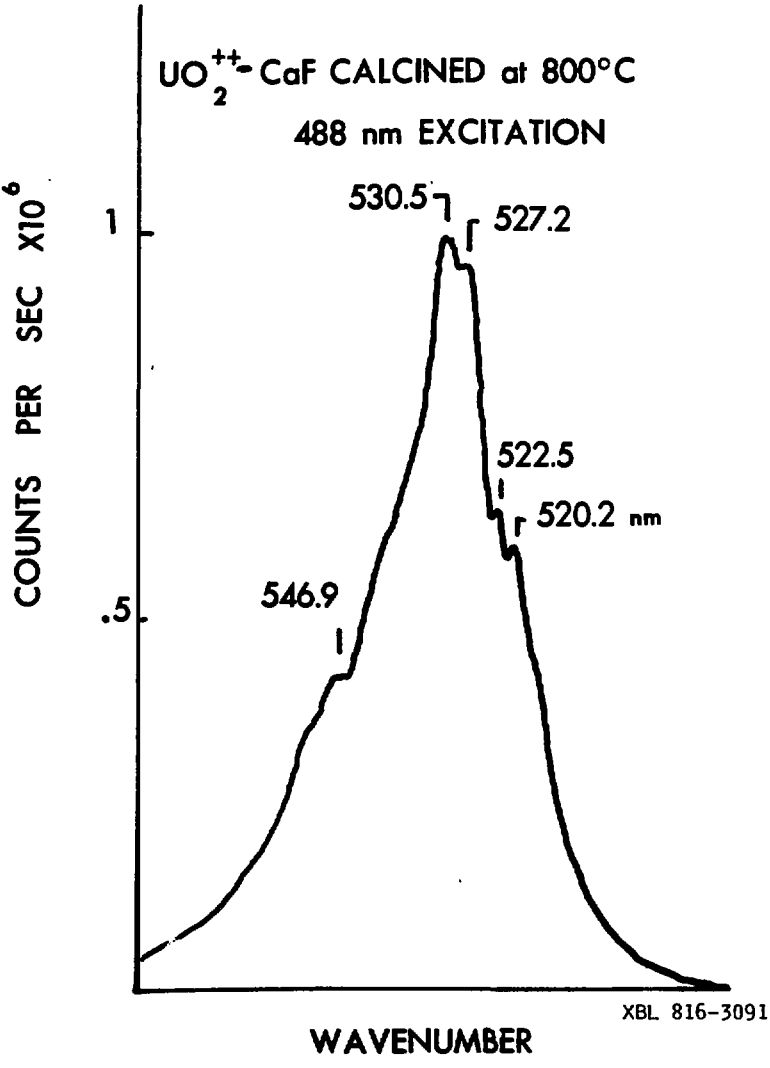

Fig. 7. Fluorescence Spectrum of 10^{-5} M UO_2^{2+} Coprecipitated with CaF_2

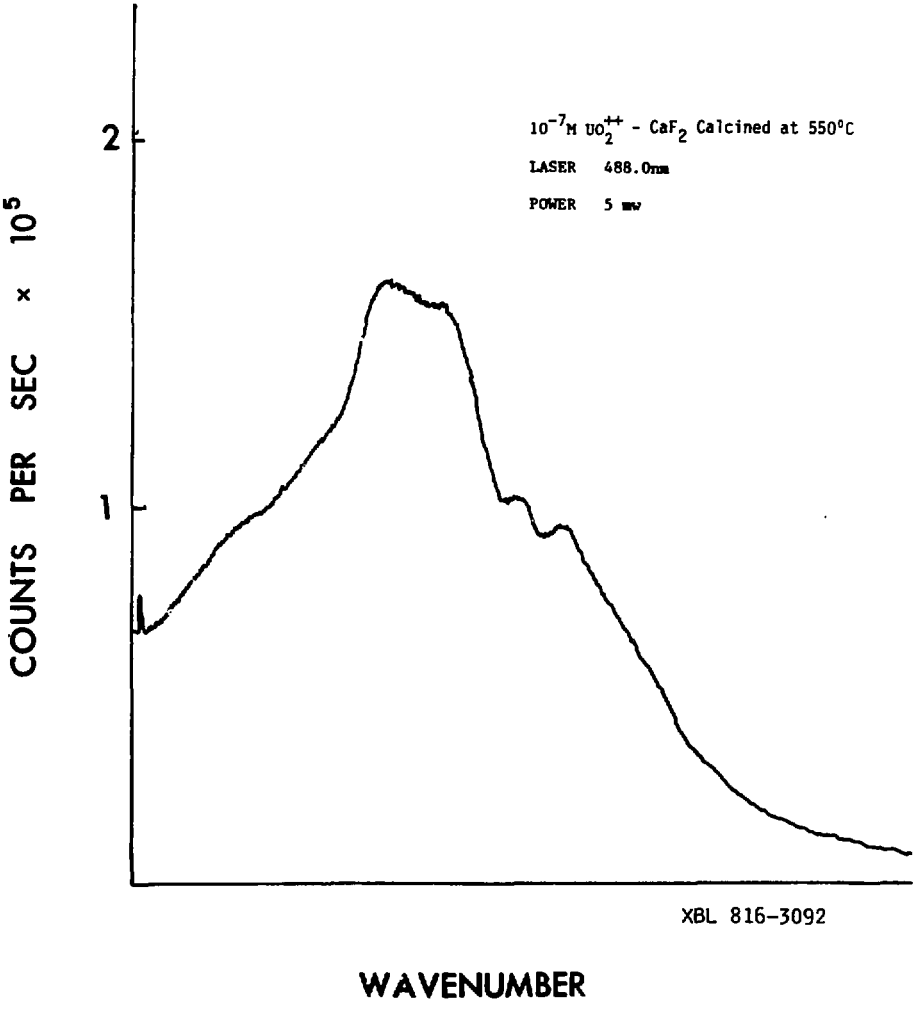

Fig. 8. Fluorescence Spectrum of 10^{-7} M UO_2^{2+} Coprecipitated with CaF_2

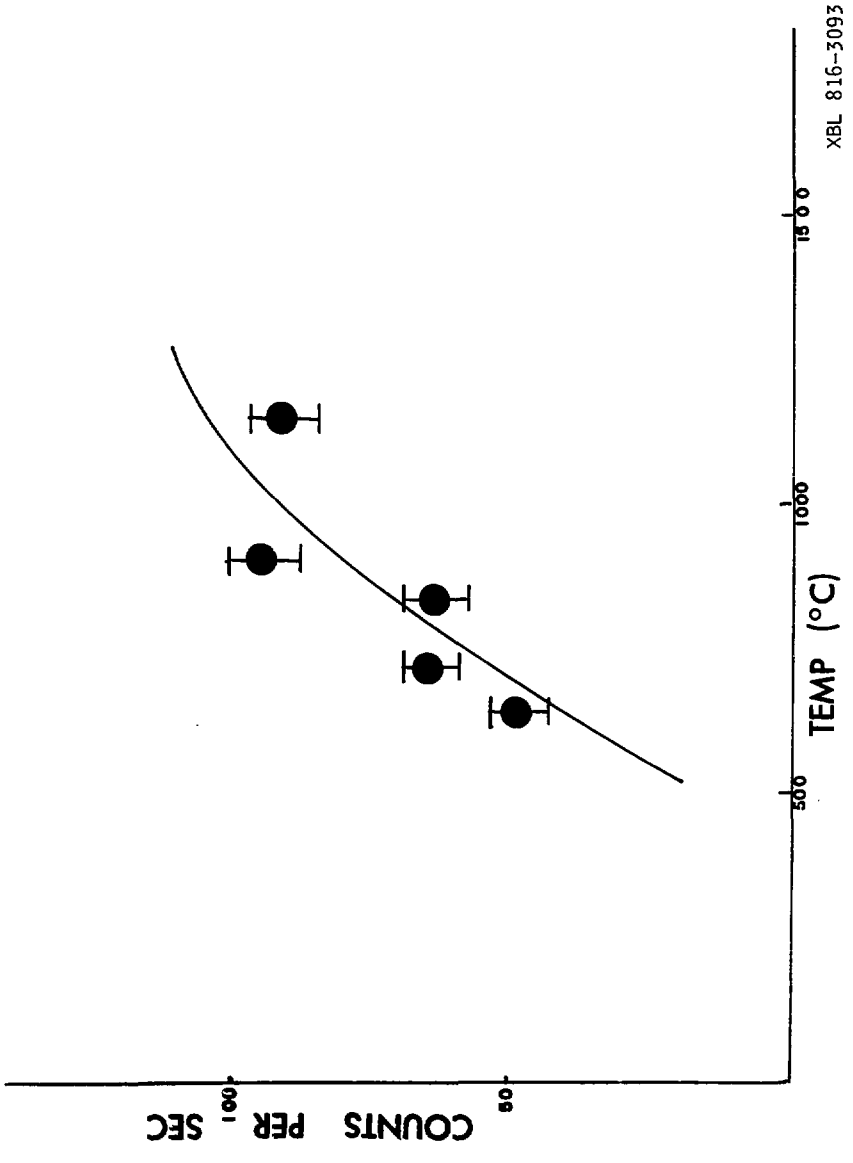

Fig. 9. UO_2^{2+} - CaF_2 Response as a Function of Calcination Temperature

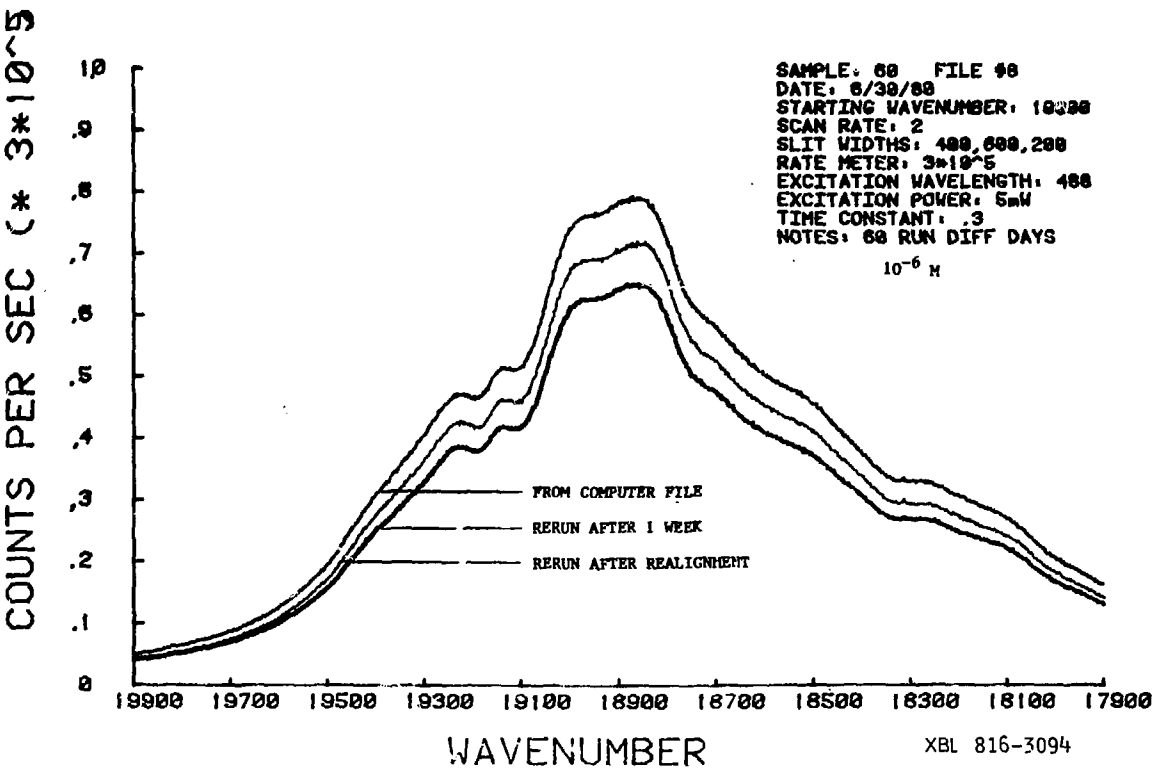

Fig. 10. Dependence of Fluorescence Response of UO_2^{2+} - CaF_2 on Instrument Alignment

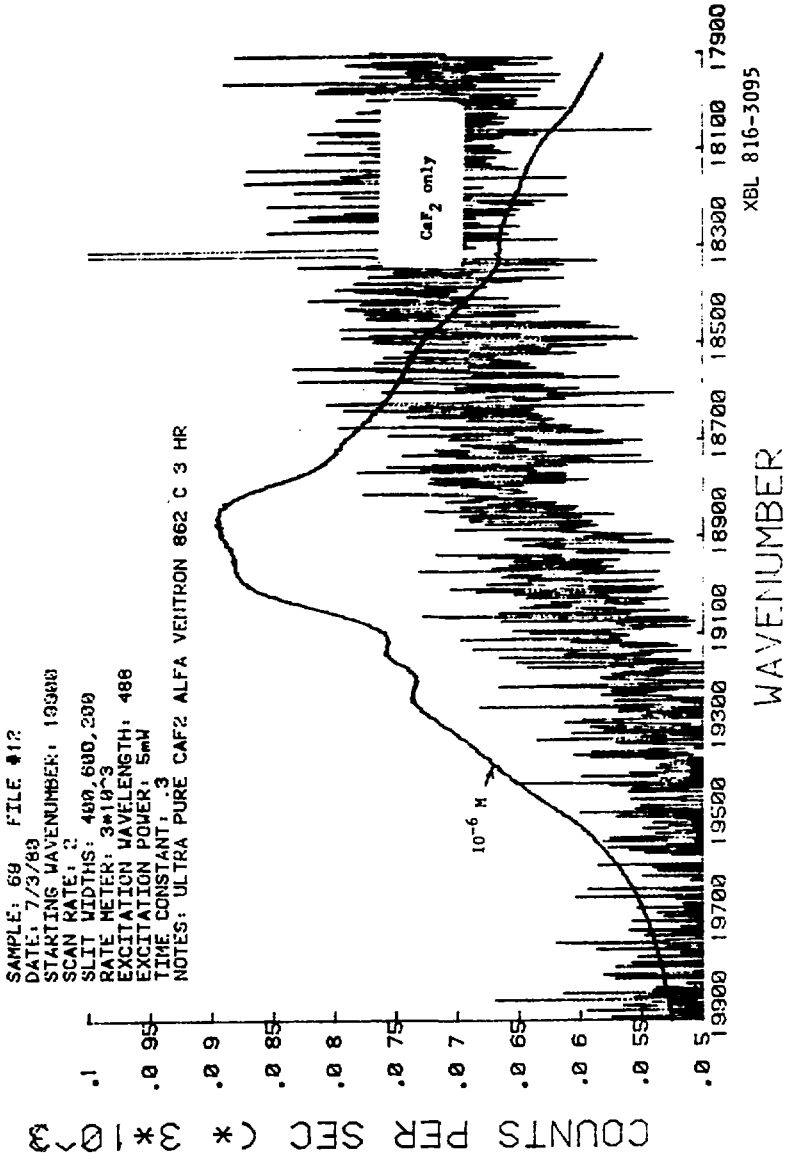

Fig. 11. Fluorescence Background and Noise Content of Coprecipitation Reagents with No UO_2^{2+}

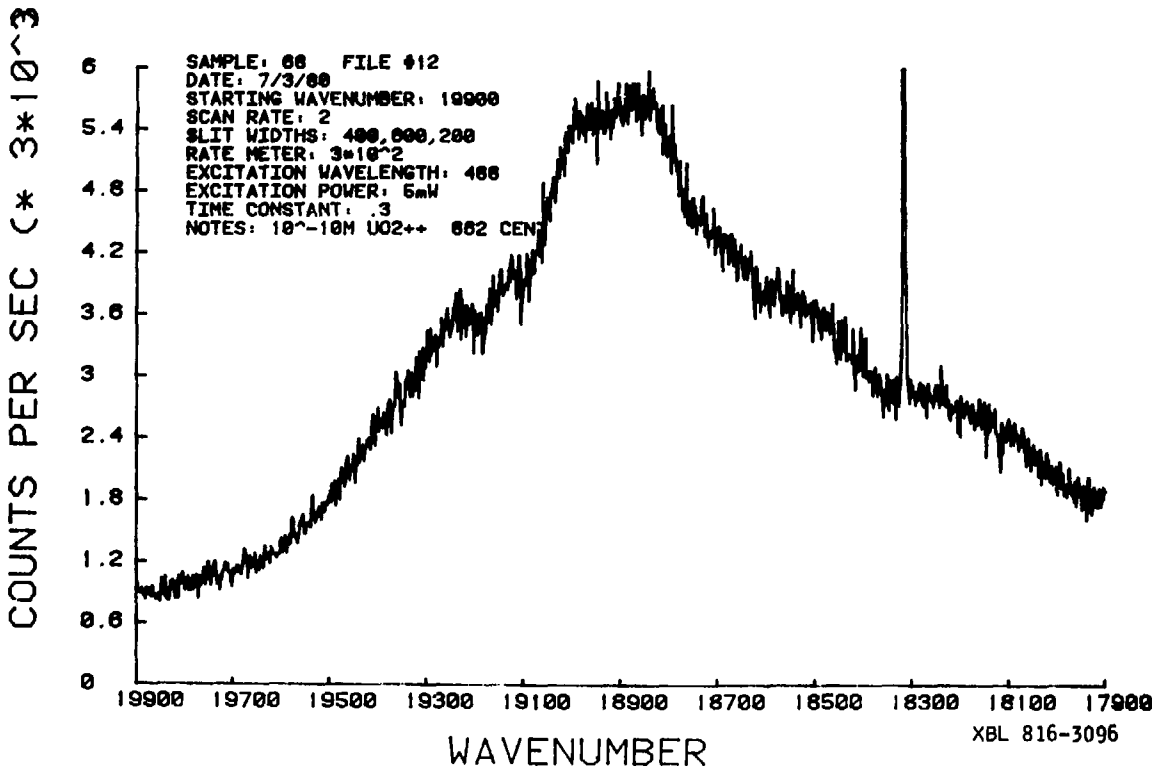

Fig. 12. Fluorescence Spectrum of 10^{-10} M UO_2^{2+} Coprecipitated with CaF_2

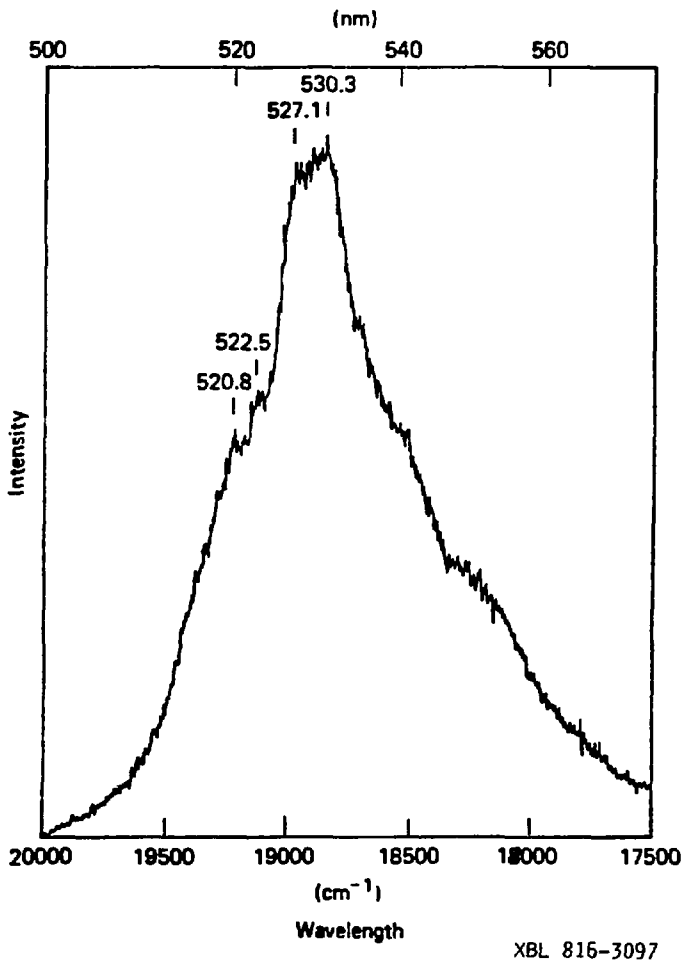

Fig. 13. Fluorescence Spectrum of 10^{-12} M UO_2^{2+} Coprecipitated with CaF_2

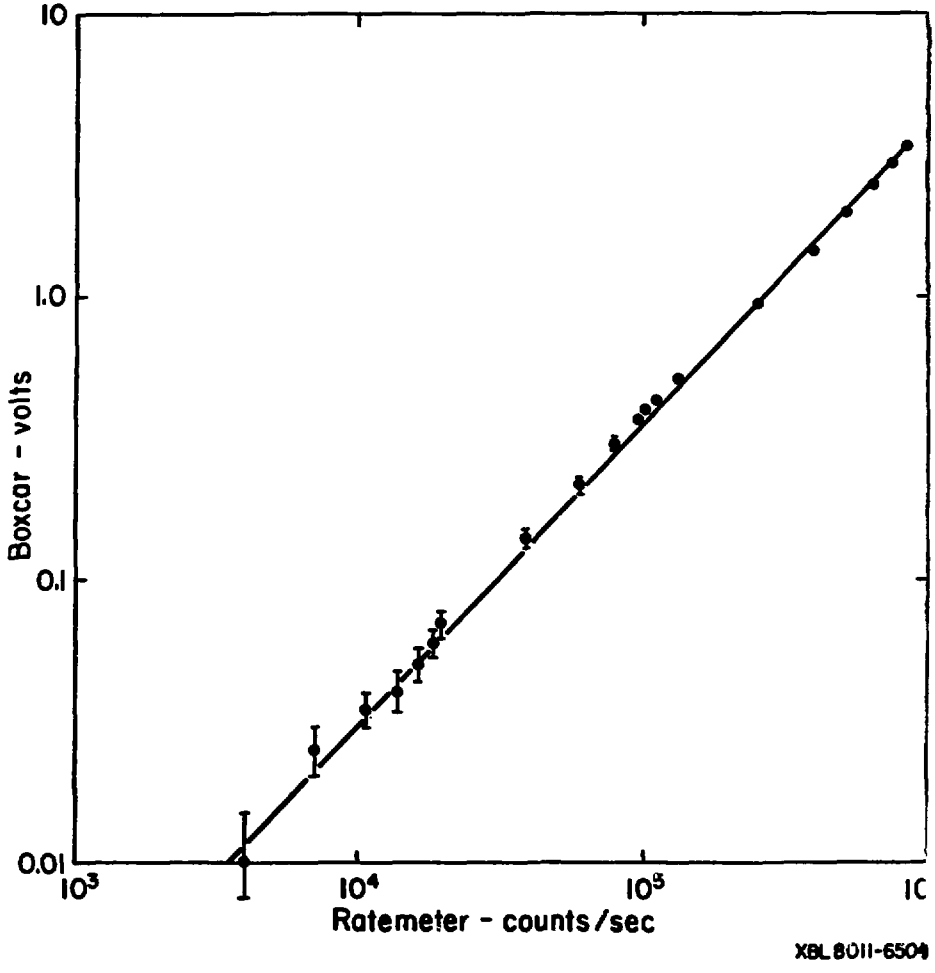

Fig. 14. Boxcar Averager Voltage vs. Ratemeter Countrate

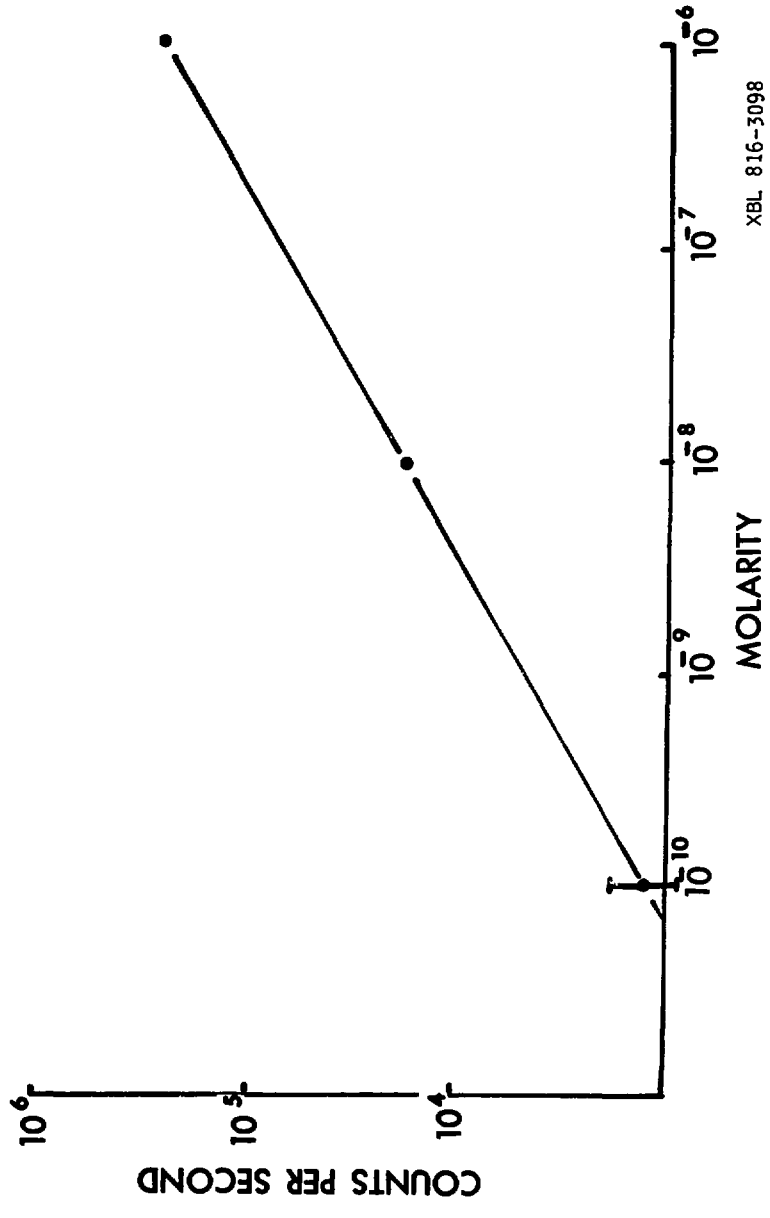

Fig. 15. Fluorescence Intensity vs. Molarity for U^{2+} Coprecipitated with CaF_2

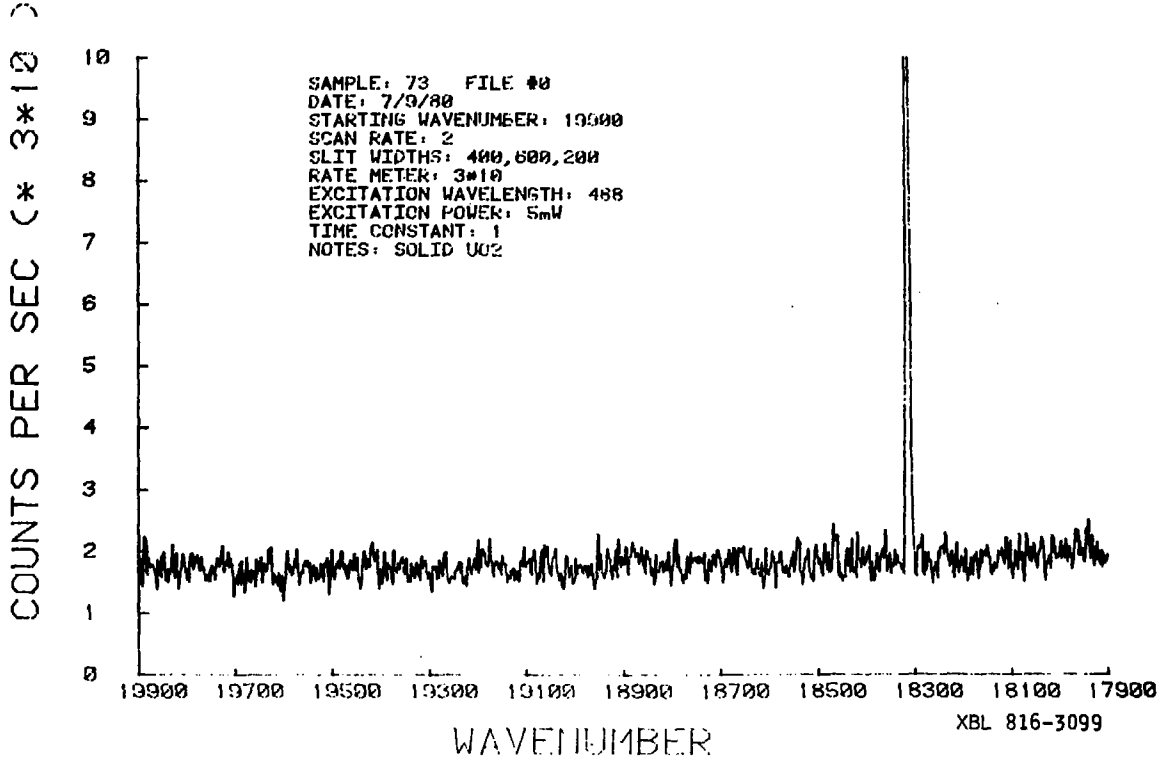

Fig. 16. Fluorescence Spectrum Solid UO_2

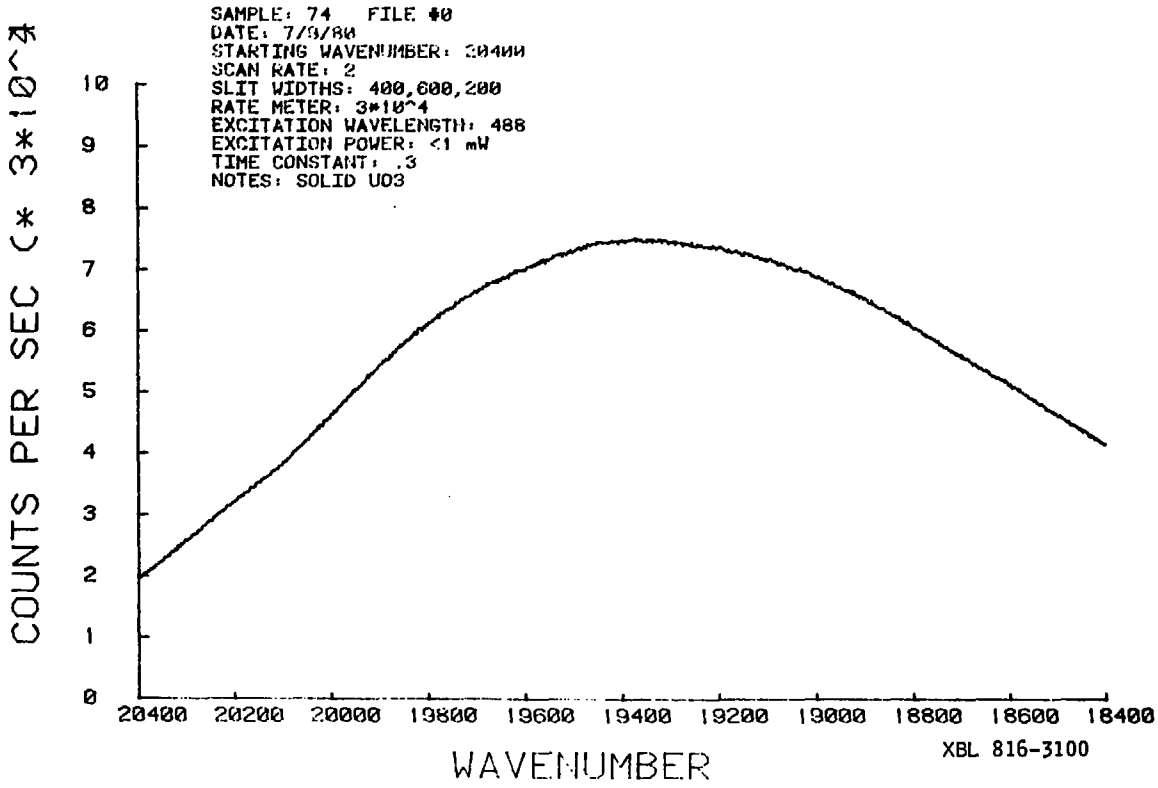

Fig. 17. Fluorescence Spectrum of Solid UO_3

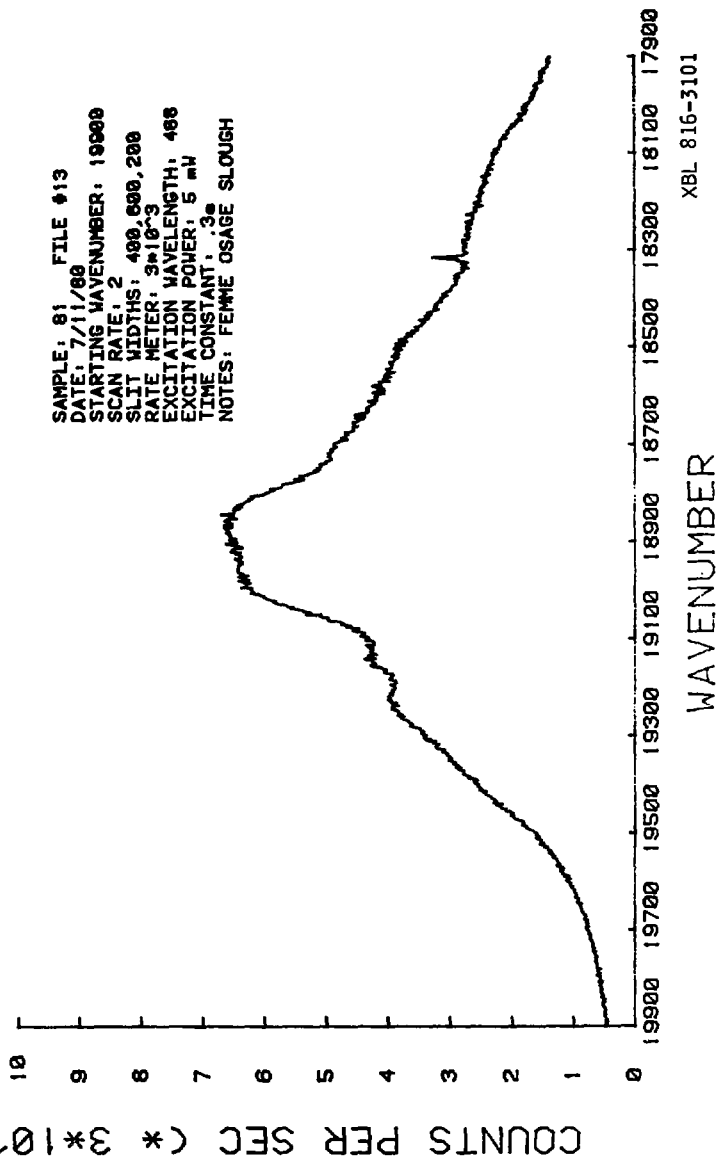

Fig. 18. Fluorescence Spectrum from Uranium in the Femme Osage Slough (63ppb)

Appendix I

Contribution from

Dale L. Perry, Stanley M. Klainer*, and Harry R. Bowman
Earth Sciences Division, Lawrence
Berkeley Laboratory, University of
California, Berkeley, CA 94720

and

Fred P. Milanovich, Tomas Hirschfeld, and Steven Miller
Chemistry and Environmental Science Divisions
Lawrence Livermore Laboratory, University
of California, Livermore, CA 94550

ULTRA-TRACE DETECTION OF URANIUM IN AQUEOUS SAMPLES BY LASER-INDUCED FLUORESCENCE EXCITATION (LIFE)

Key words and terms: uranium analysis,
laser-induced fluorescence,
selective laser excitation,
fluorescence

(Submitted to Analytical Chemistry, October 17, 1980)

ABSTRACT

A new method of analysis for ultra-trace quantities of uranium in aqueous samples has been developed with a detection limit of 4×10^{-14} M (10^{-5} ppb, 0.01 pg/mL). This detection level is considerably less than the average concentration of 0.1 ppb uranium found in natural groundwaters. The procedure consists of an initial co-precipitation of the solution uranium with calcium fluoride, calcination at 800°C, and monitoring the uranium content by laser-induced fluorescence excitation (LIFE). Analytical data using this technique are presented for previously analyzed groundwater samples containing 10^{-6}-10^{-7} M uranium. The fluorescence yield dependence on calcination time and temperature and on cation and anion interferences is discussed.

INTRODUCTION

The ability to rapidly and conveniently determine extremely small quantities of uranium in the geologic environment is desirable from several standpoints. Recent emphasis on more complete understanding of the migration of actinide materials through soils and various types of mineral deposits (especially around nuclear waste repositories) requires rapid, high sensitive analytical techniques. Hydrogeochemical exploration for uranium also requires routine analysis at very high sensitivity of a large number of samples in order to detect the presence of uranium ores through the groundwater concentration gradients they induce. Finally, an accurate and precise determination of uranium trace levels in geologic surroundings is important for basic geophysical research in radiometric age dating and terrestrial heat-flow phenomena.

Several methods of analysis for uranium have been reported in the chemical literature (1), many of which involve initial separation or enrichment techniques. The technique reported here (2) has considerably lower detection limits for the determination of uranium but is still simple enough for routine laboratory use. It involves a coprecipitation of the UO_2^{2+} ion from solution in a CaF_2 matrix and subsequent sample preparation closely patterned after those used by Wright and co-workers (3-5) in their study of lanthanide ion substitution in a CaF_2 crystal. This is followed by air calcination of the precipitate at elevated temperatures. The co-precipitated uranium is then spectroscopically monitored by laser-induced fluorescence excitation (LIFE).

This report describes the technique used for the co-precipitation of uranium in calcium fluoride matrices, experimental parameters (such as calcination temperature and time, initial uranium concentration in solution, and interfering cations and anions) that affect the concomitant fluorescent yield, spectra, and intensity of the samples, and the instrumentation used to obtain the spectra. Detection limits, uranium co-precipitation efficiency, and selectivity are discussed, along with the results of the application of the technique to actual uranium-containing groundwater samples.

EXPERIMENTAL

Reagents

Reagent purity is crucial at these concentration levels, and a number of reagents were evaluated for background uranium content. The combination of reagent grade Matheson, Coleman & Bell NH_4F and Mallinckrodt $Ca(NO_3)_2.4H_2O$ with quartz distilled, de-ionized water is required to

achieve 10^{-12} M background levels. Reagent grade $Mg(NO_3)_2 \cdot 6H_2O$ (Mallinckrodt), NaCl (Mallinckrodt), $Na_2HPO_4 \cdot H_2O$ (J. T. Baker), and $NaCO_3$ (Mallinckrodt) were also used. A stock solution of 5×10^{-3} M $UO_2(NO_3)_2 \cdot 6H_2O$ was prepared in distilled, de-ionized water and discarded whenever turbidity appeared.

Apparatus

All spectra were taken on a laser excited fluorescence spectrometer (Figure 1) employing a Spectra Physics Model 165 argon ion laser. The laser was coupled via a set of beam redirector mirrors to a Claissen filter to isolate the desired excitation wavelength, and focused into a specially made Spex right-angle optical bench containing an f/1.2 collection lens. The lenses were aligned to generate a 100 μm diameter common focus in a sample holder inclined at 45°. The collected light was refocused at f/8 into a Spex No. 14018 (0.75m focal length) double monochromator equipped with holographic gratings blazed at 500nm. The monochromatized light was re-imaged at f/2 onto a cooled (-20°C) RCA C31034A GaAs photomultiplier (PMT) in a Products for Research RF-TSA cooled housing. The PMT was operated at <2000 volts using a Power Design 2K-15 adjustable filtered HV source. The photoelectron pulses were conditioned, windowed, and counted by a photon counting system consisting of Ortec Model 9301 and 9302 amplifiers and an Ortec Model 9349 ratemeter or a Princeton Applied Research Model 162 boxcar integrator. The output of the ratemeter or boxcar was fed to a Hewlett Packard Model 3456A electrometer having an HPIB interface and controlled by a Tektronix Model 184 Time Mark Generator. The electrometer was in turn coupled to a Tektronix Model 4051 graphics processor having a flexible disk attachment, a Tektronix Model 4631 hardcopy generator,

and a Tektronix Model 4662 plotter. All the spectra used for analyses were taken using an excitation wavelength of 488 nm and an excitation power of 65 microwatts except where noted.

Uranium tracer studies were performed using a Packard Model A4606 Scintillation Counter.

Procedure

All glassware was pre-washed with dilute nitric acid followed by repeated rinsing with quartz-distilled water in order to remove any possible contaminant metal ions on the glass surfaces. One mL of a $UO_2(NO_3)_2 \cdot 6H_2O$ solution of appropriate concentration was added to a 250 mL beaker with 5 mL of 1M $Ca(NO_3)_2 \cdot 4H_2O$ and 14 mL of distilled, de-ionized water. Thirty mL of a 0.3 M NH_4F solution was then added dropwise with a magnetic stirring bar over a period of 55-60 seconds, giving a final solution volume of 50 mL. For cation and anion interference studies, the appropriate volume of quartz triply distilled water was replaced with an equal volume of cation or anion solution of known concentration holding the total volume constant at 50 mL. All solution concentrations of metal ions were expressed with respect to the final solution volume prior to precipitation. The above solutions were then covered with "Parafilm" and allowed to precipitate and settle for one day. The CaF_2 precipitates were centrifuged and dried in the centrifuge tubes at 105°C for two hours. The precipitate was removed from the walls of the centrifuge tubes with a stainless steel spatula and crushed. The samples were fired in porcelain crucibles for three hours (usually at 800°C) (Lindberg Model 51333 box furnace accurate to $\pm$ 1°C), allowed to cool to room temperature in the open air, and crushed

again in a vibrating ball mill (a mortar and pestle were initially employed, but the vibrating ball mill produced a more homogeneous powdered sample and better reproducibility in the spectra). The CaF_2 samples were then pressed into 200 mg pellets one centimeter in diameter and one millimeter thick.

RESULTS AND DISCUSSION

A number of workers have studied the luminescence of uranium in CaF_2. Lupei and Lupei (6) reported a phosphorescent spectrum exhibiting a zero-phonon line centered at 521.25 nm (19184 cm^{-1}) with associated vibronic side structure. Their studies indicated that the luminescent species most probably has a distorted octahedral UO_6^{6-} structure. Nicholas (7) reported a concentration dependent luminescence. At low concentrations of uranium, a spectrum Nicholas called Type I was observed with a no-phonon line at 521.40 nm (19179 cm^{-1}) and an equally intense line at 520.02 nm (19230 cm^{-1}). At approximately 1% uranium concentrations, Nicholas reported a spectrum dominated by lines at 528.09 nm (18936 cm^{-1}) and 527.09 nm (18972 cm^{-1}). According to Nicholas, these lines are due to uranium clustering and are called Type II spectra. Lines contained in the Type I and II spectra appear as pronounced bands in the fluorescence emission spectra obtained in this work (Figure 4).

In the present study, the fluorescence yield of coprecipitated and calcined uranium was measured at nine excitation wavelengths from 457.9 nm to 568.2 nm using a combination of Kr ion and Ar ion lasers as the excitation source. The maximum fluorescence yield occurred at 488.0 nm which was therefore chosen as the excitation wavelength for this work.

Laboratory samples were prepared containing uranium as the uranyl ion in the 10^{-4} - 10^{-12} M concentration range. Precipitates taken from solutions of 10^{-5} M and lower uranium concentrations yielded white solids and gave excellent fluorescence spectra, whereas larger concentrations gave yellow precipitates which exhibited very poor fluorescence. CaF_2 samples that have undergone no high-temperature calcination gave only a minimal, diffuse fluorescence signal.

In the working concentration range of 10^{-5} - 10^{-12} M, several experimental parameters that could influence the intensity of the fluorescence were investigated. First, a log-log plot of fluorescence intensity vs. the molarity of the uranium contained in the initial, un-precipitated solution yielded a linear calibration from 10^{-6} to 10^{-12} M. Second, the intensity of the spectrum was independent of calcination temperature in the 500-800°C range, with a slight increase at 1000°C. Third, prolonged heating of samples (up to 48 hrs) at any one-temperature had only a minimal effect on the intensity of the fluorescence emission.

The interference of other ions was investigated over a wide range of concentrations. Interference was observed for these ions at and above the following concentration levels: Fe^{3-}, 10^{-5} M; Mg^{2+}, 10^{-5} M; Al^{3+}, 10^{-5} M; Mn^{2+}, 10^{-3}M; Na^{+}, 1 M; SO_4^{2-}, 10^{-2} M.

The coprecipitation yields at various uranium concentrations were determined using tracer quantities of ^{233}U and standard scintillation counting techniques. The co-precipitation efficiency is shown in Fig. 3 and appears to be linear over the uranium concentration range of 10^{-5} M (2.7 ppm) to 10^{-8} M (2.7 ppb). About 84% of the solution uranium is coprecipitated with the CaF_2 at 10^{-5} M and 88% at 10^{-8} M uranium.

The chemical yield drops off at higher concentrations, and the overall results of the measurements become less reproducible.

Figure 2 shows the fluorescence spectra of a 10^{-12} M uranium and a reagent blank sample compared with the spectrum of a 10^{-8} M uranium sample. These three spectra were obtained with continuous wave laser excitation using the apparatus of Figure 1. The spectra of the 10^{-12} M and reagent blank sample, while indicating features of the 10^{-8} M spectrum, were considerably distorted by contributions from other sources. The distortion was removed (Figure 4) by using delayed sampling techniques (chopped excitation and boxcar integration) indicating that it was due to prompt (<50 μsec) processes such as scattering, Raman, and short lived fluorescence. Therefore the long lifetime of the uranium fluorescence (170 sec at room temperature for samples used in this work) can be effectively used to discriminate against contributions from other processes which become competitive in measurements performed at ultra-trace concentrations.

The spectrum of 10^{-12} M uranium (Figure 4), which was obtained with a time constant of 0.3 sec, exhibits a signal/noise ratio of approximately 30. By using a 10 sec time constant and accepting a signal/noise ratio of 7, a detection limit of 4×10^{-14} M is achievable. This sensitivity is superior to that of radioactive counting. The relative sensitivity of these techniques can be shown by comparing excited state lifetimes which yield <<1 photon/atom/ year for even highly radioactive actinides versus >1 photon/atom/millisecond for their fluorescent species. This difference is further compounded by the greater ease with which an atom (or molecule) can be recycled through the excited state in fluorescence measurements.

The fluorescent technique, however, is extremely sensitive to contamination, which significantly reduces its utility in many applications. This liability is greatly diminished in the present method by the coprecipitation which concentrates the UO_2^{2+} 50-100 times from solution while rejecting most solution impurities. The calcination further enhances the sensitivity by destroying most organic contaminants and increasing the quantum efficiency of the uranium.

Three surface water samples from a natural slough were analyzed using the present technique. High uranium concentrations (320 $\pm$ 30, 162 $\pm$ 20, and 65 $\pm$ 6 ppb) had been detected in these filtered (0.45 micron filter) water samples in a previous study (8). Other elements determined in these samples and their concentration ranges (in mg/mL) were: B, .08-.09; Li, 003-.005; Na, 9-15; Mg, 14-21; Al, $\sim$ 01; SiO_2, 6-10; P_2O_5, .2-3; SO_4^{2-}, 11-12; Cl, 5-6; K, 5.5-6.8; Ca, 50-70; Mn, 003-.160; Zn, $\sim$ .01; Sr, .23-.27; Mo, .04-.05; As, .14-.17; HCO_3^-, $\sim$ 240.

The laser measurements in the present work indicated uranium levels of 350 $\pm$ 30, 200 $\pm$ 20, and 63 $\pm$ 5 ppb, respectively, in aliquots taken from the stored samples above. The agreement is quite good, considering the long storage period (ten months) between the two sets of uranium determinations. These measurements were undertaken to see if any unknown interference problems would be encountered in the analysis of natural water samples.

CONCLUSIONS

A new method for determining uranium concentrations in aqueous solutions has been developed which uses a continuous argon laser to excite room temperature fluorescence in uranium that has been copreci-

pitated with CaF_2. The method has been applied to natural water samples where the uranium concentrations ranged from 10^{-6}–10^{-7} M.

The technique was demonstrated to be effective down to a uranium concentration of 10^{-11} M (2.7 pg/mL). Samples in the range of 10^{-12} M (.27 pg/ml) were analysed using a delayed fluorescence mode. The method is similar to that developed by Wright (3) for lanthanide analysis and probably can be extended to the other actinides. The detection limit of the presently described technique for uranium is 4×10^{-14} M (10^{-5} ppb, 0.01 pg/mL). This limit could be lowered considerably by utilizing preconcentration techniques and an optical system designed specifically for this type of analysis.

LITERATURE CITED

1. Campen, W.; Bachmann, K. Mikrochim. Acta 1979, 2, 159-170.
2. Milanovich, F.; Hirschfeld, T.; Klainer, S. M.; Perry, D., Second Chemical Congress of the North American Continent and the 180th National Meeting of the American Chemical Society, Las Vegas, Aug. 24-29, 1980.
3. Wright, J. C.; Gustafson, F. J., Anal. Chem. 1978, 50, 1147A-1160A.
4. Miller, M. P.; Tallant, D. R.; Gustafson, F. J.; Wright, J. C., Anal. Chem. 1977, 79, 1474-1482.
5. Wright, J. C.; Johnston, M. V., Anal. Chem. 1979, 51, 1774-1780.
6. Lupei, A.; Lupei, V. J., Phys. C: Solid St. Phys. 1979, 12, 1123-1130.
7. Nicholas, J. V. Phys. Rev. 1967, 155, 151-156.
8. Strisower, B. Lawrence Berkeley Laboratory Report No. LBID-152, University of California, Berkeley, CA, January, 1980.

ACKNOWLEDGEMENTS

This research was supported by the U. S. Department of Energy under contract W-7405-ENG-48 and the Office of Nuclear Waste Isolation through Program No. E511-09800. The authors wish to thank Professor John Wright of the Department of Chemistry, University of Wisconsin, for helpful discussions.

FIGURE CAPTIONS

Figure 1. Schematic diagram of the photon counting spectrofluorometer used in this work.

Figure 2. Fluorescence spectra of 10^{-12} M UO_2^{++}, 10^{-8} M UO_2^{2+}, and reagent blank samples. The 10^{-12} M and reagent blank were taken with 1 mW laser power, 488 nm excitation, and 3s time constant. The 10^{-8} M spectra was taken with 65μw and .3s time constant.

Figure 3. Coprecipitation efficiency vs. the log of uranium molarity.

Figure 4. Fluorescence spectrum of 10^{-12} M UO_2^{++} sample taken with boxcar integration. Laser power, 150 mW, time constant, .3s laser pulse width, 500 s; boxcar delay, 50μs; and boxcar integration width, 50μs.

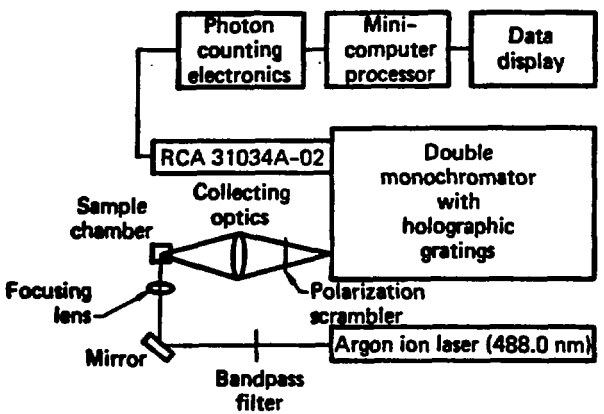

Fig. 1. Schematic diagram of the photon counting spectrofluorometer used in this work.

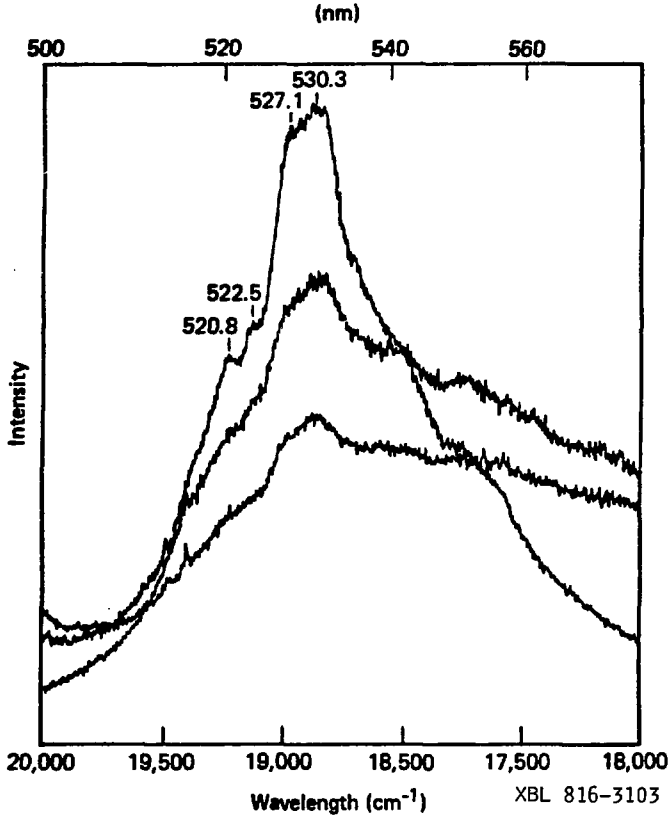

Fig. 2. Fluorescence spectra of 10^{-12} M UO_2^{++}, 10^{-8} M UO_2^{2++}, and reagent blank samples. The 10^{-10} M and reagent blank were taken with 1 mW laser power, 488 nm excitation, and 3 s time constant. The 10^{-8} M spectra was taken with 65μw and .3s time constant.

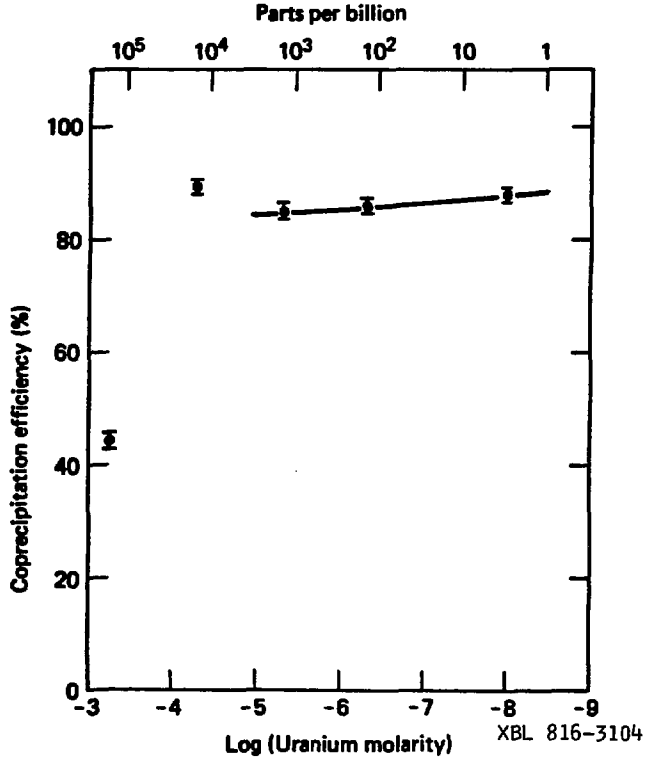

Fig. 3. Coprecipitation efficiency vs. the log of uranium molarity.

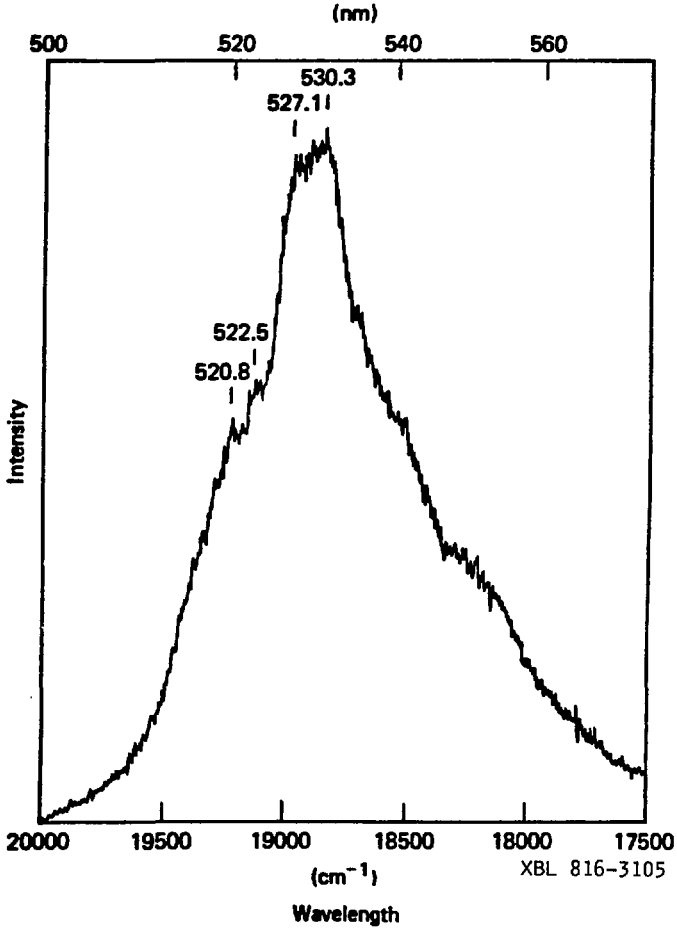

Fig. 4. Fluorescence spectrum of 10^{-12} M UO_2++ sample taken with boxcar integration. Laser power, 150 mW, time constant, .3 s laser pulse width, 500 s; boxcar delay, 50μs; and boxcar integration width, 50μs.

Appendix II

REMOTE FIBER FLUORIMETRIC ANALYSIS

Improvements in optical fibers now make it possible to send laser pulses and receive fluorescent light signals over distances of up to a kilometer. We have been developing laser fluorimetry as a laboratory tool of great versatility and sensitivity for chemical analyses, and these improved optical fibers enable the fluorimeter to remotely sense in environments too hostile, hazardous, or inaccessible for normal instrumentation. Besides having a wide range of possible applications in industry and research, remote fibler fluorimetric analysis may also be applied in multiple-site monitoring from a central location over a switchable fiber-optic network. We are developing an instrument based on remote analysis to be used as an in situ monitor for rare-earth-ion transport in a nuclear-waste repository. We are also exploring further applications as advances in the technique are made possible by new developments in laser-induced fluorescence and in fiber-optical technology.

Modern technology is crucially dependent on analytical monitoring and control, but there are many cases in which this analysis is best done from a distance.[1,2] Locations such as an underground nuclear-waste-disp;osal site, or the working zone of a coal-liquifaction reactor are much too hostile for most in situ analytical devices.

Hitherto, these situations called for the development at considerable expense and delay of specially durably made instruments or when when possible, of equally rugged sampling systems that could collect a representative sample and deliver it to the instrument without

alteration. Instead of these very often extensively development programs, the possibility of designing instruments to perform analyses remotely appeared as a welcome alternative.

Analytical fluorescence spectroscopy

A fluorescence spectroscope functions by exposing a chemical sample to laser light and measuring the wavelengths re-radiated. The specific wavelengths are characteristic of the emitting substance, and their intensity is proportional to its concentration in the sample. Thus, in many cases the fluorescence spectroscope can simultaneously tell us what is in the sample and how much is present.[3]

Existing fluorescence spectrometers require the sample to be present in an optical cell within the instrument. To convert the instrument for remote analyses, we first needed to find a way to transmit the fluorescent light back to the spectroscope efficiently. The simultaneous development of optical fibers for the telephone and computer insustries and of laser-induced fluorescence for high-sensitivity chemical analysis made it possible for us to build such a remote analysis device.

The communications industry, faced with a need to transmit signals of greater bandwidth accommodated on electrical cables, developed fiber-optic that can transmit light over distances of up to a kilometer with remarkably little alteration.[4] They also created a whole new technology of special connectors, multiple couplers, and input-output optics that made such "light wires" no harder to use than coaxial cable. Successive technological advances have enlarged the wavelength range of such fibers, until they now cover most of the visible and a good portion of the near infrared spectrum.

We have recently improved the sensitivity of analytical fluorescence spectroscopy by using lasers as an illumination source that is extremely bright, spectrally pure, and controllable.[3] We have so far demonstrated parts-per-trillion sensitivities in the detection of many chemicals. A further virtue of the laser, its ability to be focused within an extremely small spot, has made it possible to illuminate the small entrance aperture of a long-distance optical fiber and has suggested the present work.

Remote fiber fluorimetry

We first demonstrated the feasibility of using these technological developments by coupling separate fibers to a laser source and to a photomultiplier in the spectrometer.[5] We brought the far ends of the fibers together at an angle, as shown in Fig. 1a. The sensitive volume (shaded) is defined by the overlap of the fields of view of the two fibers.

Figure 1b shows the probe in use on a sample of water containing 10ppm of rhodamine-6G, which it illuminated with several milliwatts of green light from a laser 100m away. The fluorescence signal at the photomultiplier, also 100 m away, was several hundred thousand counts per second. Surprisingly, sunlight made only a minor background contribution, because the fiber has a very low acceptance for any light source less intense than a laser.

This system, however, is far from optimal. Calculations show that only a small fraction of the fluorescence from the overlap volume will be collected by the fiber. To improve the collection efficiency, we added a beamsplitter at the instrument end to permit us to send the

laser light and receive the fluorescence signal through the same fiber (Fig. 2a). The other end of the fiber illuminates and collects light from the shaded volume indicated in Fig. 2b.

To be useful for chemical analyses, such a system should have a linear response function. Figure 3a shows the response to a set of rhodamine-6G solutions at different concentrations; a 100:1 beam attenuator is used to avoid saturating the detector. The calibration curve is linear from at least 0.1 to 10ppm, and a detection limit of about 10ppb was confirmed by actual measurement (Fig.3b).

A mathematical analysis of the behavior of this fiber-optical sensor probe showed that its signal level is directly proportional to its diameter. Since we were using commercial fibers developed for other purposes, there was no simple way to increase the fiber diameter. We achieved almost the same effect, however, by adding a lens in front of the fiber.

Figure 4a shows a particularly simple version of this idea, which includes a glas or sapphire ball cemented in the end of a glass tube. During assembly we send laser light through the fiber, observe the resulting beam, move the fiber lengthwise to find the best focus, and then hold it in that position until the cement sets. Figure 4b shows the probe sending a beam of green laser light (note the spot of light on the palm of the hand) through a fluorescent sample. The same ball lens collects the yellow fluorescence light and focuses it into the fiber for transmittal to the photomultiplier of the fluorescence spectrometer.

With such a standardized probe, it becomes possible to compare the response of the system to a variety of fluorescent compounds.

Table 1 lists signal levels from a number of materials, each at a concentration of 10 ppm, measured at the end of a fiber 100 m long.

The technology of remote fiber fluorimetry

One of the by-products of the fiber-optic technology developed by the communications industry is the ability to connect many fibers in parallel or in sequence to a single source. This in turn allows a remote fiber fluorimeter to monitor a number of measurement points with a single instrument. Figure 5 is a block diagram of such a device.

Since each of the fibers may be up to 1km long, this scheme allows a single instrument to provide continuous or rapid sequential analysis of many points, throughout an entire waste disposal site or refinery, for example.

For routine in situ sampling, it would be necessary to provide special lead-through holders for the probes. For occasional or temporary hand-held optrode (the optical analogue of an electrode) would suffice. Either way, the probe is quite insensitive to position. All the critical alignments are inside the probe, locked in place during assembly.

We are currently developing such a multipoint sensor system in conjunction with fluorescent rare-earth tracers to monitor groundwater movement in an experimental nuclear-waste repository.[6] The glass fibers are extremely resistant to radiation damage, which gives them a unique advantage over other kinds of sensors in this application. They can also be permanently buried with the waste and monitored from the surface with no threat of being incapacitated by moisture or voltage surges.

Because of its very high sensitivity, fluorimetry has become more and more widely used in recent years. About 90% of all chemical compounds are non-fluorescent, however, and hence not directly detectable by fluorimetry. In many cases we have been able to extend the fluorimetric technique to include these compounds by finding reagents that render them fluorescent or whose fluorescence they affect.

We have incorporated this technology into remote fiber fluorimetry by coating the surface of the probe with an insoluble or covalently bound reagent. It is important, of course, to choose a reversible equilibrium reaction to avoid depletion of the reagent. Such a chemically specific optrode behaves much like an ion-specific electrode, detecting only its target compound.

Future developments

As advances in laser fluorimetry and fiber communications become available, we plan to incorporate them to extend the capabilities of this analytical technique. There are also new glasses, now under development and soon to be marketed, with extended spectral ranges that will allow us to make observations in the near ultraviolet and the intermediate infrared. These developments will broaden the range of fluorescent compounds that are suitable as indicators.

We are also looking into ways to make optrodes sensitive to a wide variety of non-fluorescent stimuli. Additional parameters for which we may be able to develop optrodes include temperature, pressure, and radiation.

Summary

We have developed a way to extend the sensing and analytical abilities of the laser fluorescence spoectrometer beyond the physical confines of the laboratory by means of communications-grade optical fibers. These fiber probes are extremely rugged, compared with sensitive laboratory equipment, and also extremely inexpensive. They make it possible to perform sensitive chemical analyses in hostile environments without risking damage to the laser and the spectrometer.

We have produced special-purpose optrodes that are sensitive to selected chemicals. With multiplexing, we can scan a number of fibers whose terminals are at widely scattered locations, gathering information in one central instrument without the expense and delay involved in manual sample-gathering.

We have begun development of a remote analyzer for monitoring rare-earth-ion migration in a nuclear-waste repository, an environment too hostile for any previous remote sensing device. We are also developing optrodes sensitive to a wide variety of non-chemical stimuli.

Notes and references

1. T. Hirschfeld, "The Instrumentation of Environmental Optics," Optical Engineering (in press)

2. T. Hirschfeld, "Methods the Laser Made Possible," 32nd Annual Symposium on Analytical Chemistry, Purdue University, West Lafayette, Indiana (1979)

3. Laser fluorescence spectroscopy for chemical analyses was described in Energy and Technology Review for January, 1978 (UCRL-52000-78-1), p. 9

4. J.E. Midwinter, Optical Fibers for Transmission (Wiler, New York, 1979)

5. T. Hirschfeld, G.R. Haugen, D.C. Johnson, and L.W. Hrubesh, "Remote Techn iques Based on Long-Distance Fiber Optics," 179th National Meeting, American Chemical Society, Houston, Texas (1980)

6. S. Klainer and T. Hirschfeld, "Trace Analysis of Ground Waters," Earth Sciences Division Annual Report, Lawrence Berkeley Laboratory, ESD-10686 (1979)

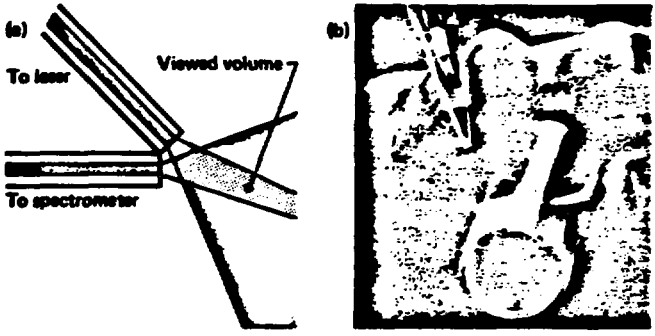

Fig. 1 *The first form of fiber termination we used for development of our remote fluorimetric analyses. Two separate fibers up to 1 km long meet at an angle at the sample, one bringing light from the laser and the other sending the fluorescence light signal to the spectrometer. (a) Schematic diagram of fiber ends, showing how the viewing cone of the spectrometer's fiber overlaps the illumination cone of the laser fiber. This region of overlap defines the sensitive volume of the probe. (b) The probe in use to examine a sample of water containing 10 ppm of rhodamine-6G. Multiple reflections in the glass vial cause the whole sample to fluoresce. The probe can be used even in direct sunlight, because the fiber accepts only a tiny fraction of the ambient light.*

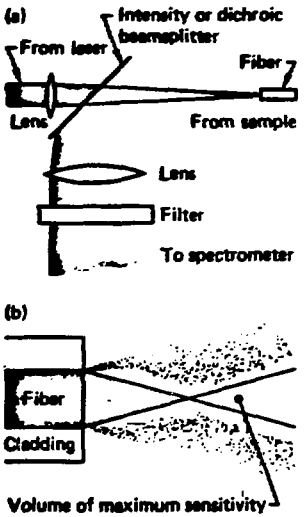

Fig. 2 *Details of a single-fiber fluorimeter, which collects light more efficiently and eliminates alignment problems at the fiber termination. (a) Schematic diagram of the beamsplitter that separates the laser illumination from the fluorescence light signal returning to the spectrometer and analyzer. (b) Sensitive volume defined by the interplay of the laser illumination region and the viewing cone of the fiber. The light-collection efficiency diminishes from a maximum in the dark-colored cone-shaped volume to zero at the outer fringes.*

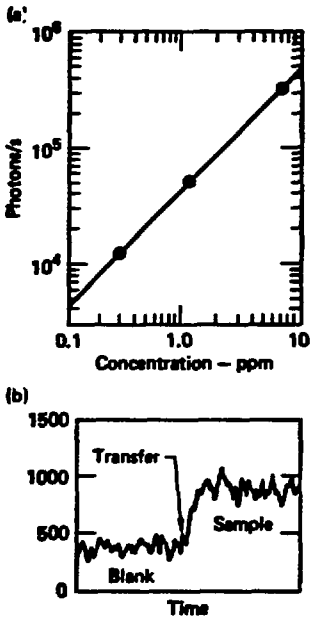

Fig. 3 *Analysis for rhodamine-6G with the remote fiber fluorimeter. A fiber probe 100 m long is used. (a) Calibration curve (measured in series with a 100:1 attenuator to avoid saturating the detector) showing the wide range of linearity. Sample concentrations were varied from 0.1 to 10 ppm. (b) Response curve documenting detection of 11 ppb of rhodamine-6G in water with light transmission through 100 m of fiber.*

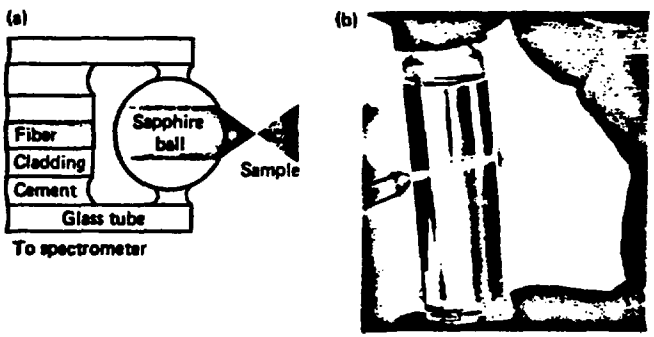

Fig. 4 *A probe with improved sensitivity and light-gathering efficiency. (a) Simplified diagram showing the optical path. The sapphire ball serves as a lens to concentrate the laser light into a beam in the sample and to collect the fluorescence light into the fiber. Optimal position and alignment of the fiber end is determined experimentally during assembly before the cement sets. (b) Green light from the laser projected by the probe through the sample and onto the palm of the hand. The yellow fluorescence light returns through the probe to the spectrometer.*

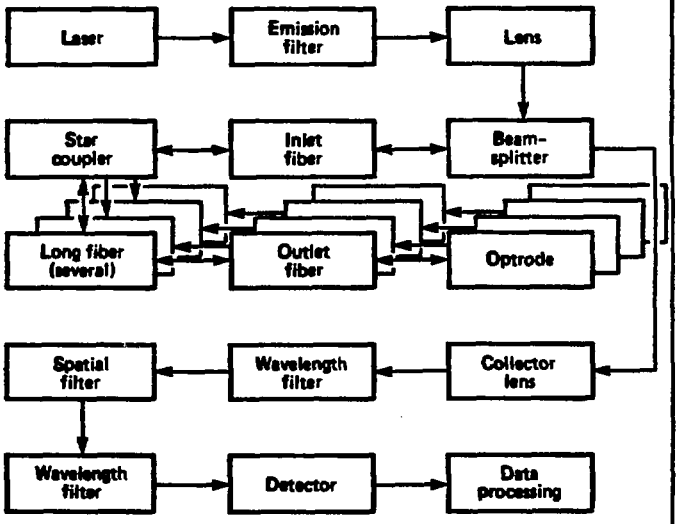

Fig. 5 *Block diagram of a remote fluorimeter equipped with multiplexing to connect it to a series of different fibers terminating at widely scattered locations. With such equipment one laser and one spectrometer could monitor the concentration of a key ingredient through all steps of a manufacturing process in a large factory or refinery. Such equipment would also permit a group of laboratories to share the expense of a single laser and spectrometer. We are developing an instrument like this to detect fluorescent rare-earth tracers specifically for monitoring groundwater movement in strategically located spots throughout an experimental underground repository for nuclear waste. The glass fibers are extremely resistant to radiation, vibration, moisture, and temperature extremes that would incapacitate other forms of remote detectors.*

Table 1 *Representative fluorescent dyes and the signals they generate at a concentration of 10 ppm in the fluorescence spectrometer with a 100-m optical fiber.*

	Photons/s
Acridine red	88 000
Rhodamine-B	380 000
Rhodamine-6G	460 000
Fluorescein	170 000
Dichlorofluorescein	90 000
Brilliant sulphoflavine	205 000
Ethidium bromide	14 000
3,3' diethylomodi-carbocyanine iodide	50 000
Th-1-amino-4-hydroxy-anthraquinone	9 000

Appendix III

SIGNAL LEVELS IN DISTAL FIBER OPTIC FLUORIMETRY

At the distal end of a fiber bundle having

d = core diameter

Na = numerical aperture

submerged in a liquid for which

n_s = liquid sample refractive index

we have

1) $$\alpha = \arcsin \frac{NA}{n_s}$$

and the effective pathlength, normalized to the exit face illumination and the full acceptance solid angle of the fiber, is

2) $$\ell_E = \frac{0.727\ d}{\tan \alpha} = 0.727 \sqrt{n_{s/NA}^2 - 1}\ d$$

The collection efficiency corresponding to this pathlength is

3) $$G = \frac{1-\cos \alpha}{2}$$

The effective photon yield at the fiber distal end then becomes

4) $$Y = M \frac{N_{av}}{10^3} C \ell_E Q_F G$$

where

M = sample molarity

N_{av} = Avogadro's number

C = sample absorption cross section

Q_F = sample fluorescent quantum efficiency

By factoring in the efficiencies of the transmission, and of the excitation and photometer optics, we get

$$5)\quad S = \left(\frac{P\lambda}{\nu c}\right) T_E T_{FE} T_I^4 \left(e^{-a_1 R}\right) \left[364.10^{-4}\, M\, N_{av}\, C d Q_F \left(\sqrt{\left(\frac{n_s}{NA}\right)^2 - 1} - \frac{NA}{\nu_s} \& \frac{n_s}{NA}\right)\right]$$

$$\left(e^{-a_2 R}\right) T_R T_{FR} Q_E$$

where

- P = illumination power
- λ = illumination wavelength
- b = Planck's constant
- C = velocity of light
- T_E = emitter transmission
- T_{FE} = excitation filter transmission
- S = signal counting rate
- T_I = fiber insertion loss
- a_1 = attenuation coefficient for excitation wavelength
- a_2 = attenuation coefficient for emission wavelength
- R = range
- T_R = receiver transmission
- T_{FR} = receiver filter transmission
- Q_E = receiver detector quantum efficiency

As an example, for

P = 1W

λ = 6741 Å

T_E = 80%

T_{FE} = 80%

T_I = 90%

R = 1000 M

a_1 = 10 lb/km

a_2 = 5 lb/km

M = 10^{-6}M

C = 10^{-19} cm^2/molec

d = 0.4 mm

NA = 0.4

n_s = 1.334

T_R = 80%

Q_F = 10%

T_{FR} = 25%

Q_E = 10%

we have

S = $1.8.10^6$ photoelectron/sec.

an easily detectable signal level.

APPENDIX IV

EXTRAPOLATION OF COPRECIPITATION-LIFE TECHNIQUE SENSITIVITY FOR URANIUM

	PRESENT	POTENTIAL	SENSITIVITY
Initial			
Count rate	1.38 KHz	40.6 KHz	29.4 X
Background	10^{-12}M	10^{-13}M	3.16 X
Concentration	10^{-10}M	10^{-16}M	10^{-6} X
Laser power	65 μW	1300 mW	20000 X
Throughput matching	50%	100%	2.0 X
System transmission	5.5%	25	4.55 X
Illuminated area	7.85×10^{-5} cm^2	7.85×10^{-2}	NA
Collection solid angle	0.366	2.96	8.09 X
Spectral bandwidth	120 cm^{-1}	400 cm^{-1}	2.0 X
Cooling	NO	YES	10 X
Time filtering	100%	10%	31.6 X
Preconcentration	NA	10	10 X
SNR (RMS)	36:1	20:1	0.55 X
Volume observed	0.001%	100%	10^{-5} X
Processed volume	50 ml	0.5 ml	100 X
Quantity sensitivity	5×10^{-17} moles	5×10^{-19}	100 X

APPENDIX V

DISTAL FLUORIMETRY VIA FIBER OPTICS: EFFECTIVE PATHLENGTH

A fiber optice guide illuminated through a dichroic beamsplitter can be used to accomplish fluorimetry at the other end of the fiber with a minimum of far end equipment. The system appears to be a promising tool for multi-point surveillance of moderately distant locations that may be fairly inaccessible.

The sensitivity of the system differs from that of a conventional fluorimeter by the losses in the fiber and by the geometrical limitation of the distal end optics.

The former can be easily allowed for, but to calculate the latter some simplifying assumptions are required.

For a sharp, perpendicular, unlensed cutoff at the distal end, the illuminating beam will be a truncated cone for which

d_o = initial diameter

θ = angular semiaperture

Here we can calculate

1) $$\alpha = \arcsin \frac{NA}{n_E}$$

where

NA = fiber numerical aperture

n_E = external medium index

Geometrical vignetting by both the spatial and the angular acceptance of the fiber divides all the illuminated space in front of the fiber in four regions.

Up to a distance

2) $$\ell_1 = \frac{d}{2 \tan \alpha}$$

.rom the exit face, the solid angle of collection will be

3) $$\Omega_i = 2\pi(1-\cos \alpha)$$

for any illuminated point in the plane normal to the axis within a circle of radius

4) $$r_1(\ell)=(\ell_1-\ell) \tan \alpha = \frac{d}{2} - \ell \tan \alpha$$

and decreasing linearly (a conservative approximation) from there to 0 at a radius

5) $$r_2(\ell) = \frac{d}{2} + \ell \tan \alpha$$

The gaussian illumination pattern can be conservatively approximated by a triangular one peaking at r = o and reading o at $r = r_2(\ell)$, thus

6) $$I(r_1\ell) = I(o,\ell) \left[1- \frac{r(\ell)}{r_2(\ell)}\right]$$

where

$r(\ell)$ = radial distance from axis at ℓ

$I(o,\ell)$ = peak intensity at center

$I(r,\ell)$ = value of intensity at a given radius and axial distance

Since

$$7) \quad P = \int_0^{r_2(\ell)} 2\pi r(\ell) I r_1 \ell \, \partial r(\ell) = 2\pi I(o,\ell) \int_0^{r_2(\ell)} r(\ell)\left[1 - \frac{r(\ell)}{r_2(\ell)}\right] \partial r(\ell)$$

where

P = total power

Now

$$8) \quad P = \frac{\pi}{3} I(o,\ell) r_2^2(\ell)$$

from where

$$9) \quad I(r,\ell) = \frac{r_2(\ell) - r(\ell)}{\pi r_2^3(\ell)} P$$

and so we have for the relative excitation efficiency

$$10) \quad \frac{I(r,\ell)}{I(o,o)} = 1 - \frac{r(\ell)}{r_2(\ell)}$$

If we normalize to a Ω, observation solid angle at the o,o location, the mean efficiency of a given constant ℓ plane will be

the mean efficiency of a given constant ℓ plane will be

$$11)\quad E(\ell) = \frac{3}{\pi r_2^2(\ell)}\left\{\int_0^{r_1(\ell)} 2\pi r(\ell)\left[1-\frac{r(\ell)}{r_2(\ell)}\right]\partial r(\ell)+\int_{r_1(\ell)}^{r_2(\ell)} 2\pi r(\ell)\left[1-\frac{r(\ell)}{r_2(\ell)}\right]\left[\frac{r_2(\ell)-(\ell)}{r_2(\ell)-r_1(\ell)}\right]\partial r(\ell)\right\}$$

$$= \frac{6}{r_2^3(\ell)}\left\{\int_0^{r_1(\ell)}\left[r_2(\ell)r(\ell)-r^2(\ell)\right]\partial r(\ell) + \frac{1}{r_2(\ell)-r_1(\ell)}\int_{r_1(\ell)}^{r_2(\ell)}\left[r^3(\ell)+r_2^2(\ell)\ r(\ell)-2r^2(\ell)r_2(\ell)\right]\partial r(\ell)\right\}$$

$$= \frac{6}{r_2^3\ \ell}\left[\frac{1}{2}\ r_2(\ell)r_1^2(\ell)-\frac{1}{3}r_1^3(\ell)+\ \frac{\frac{1}{12}\ r_2^4(\ell)-\frac{1}{4}\ r_1^4(\ell)-\frac{1}{2}\ r_2^2(\ell)r_1^2(\ell)+\frac{2}{3}\ r_1^3(\ell)r_2(\ell)}{r_2(\ell)-r_1(\ell)}\right]$$

From which

$$12)\quad E(\ell)= \frac{d^3+6d^2\ell\tan\alpha-4d\ell^2\tan^2\alpha+8\ell^3\tan^3\alpha}{(d+2\ell\tan\alpha)^3}$$

$$\ell<\ell_1$$

The substitution

$$13)\quad x = \frac{\ell}{\ell_1}$$

allows the simplification

14) $$E(x) = \frac{x^3-x^2+3x+1}{(1+x)^3}$$

$x<1$

the effective pathlength from 0 to ℓ_1 then becomes

15) $$t_{<\ell_1} = \ell_1 \int_0^1 \frac{x^3-x^2+3x+1}{(1+x)^3}\,\partial x = (\frac{7}{2} - 4\ell n2)\ell_1 = 0.727\ell_1$$

From $\ell>\ell_1$ we can again consider two radial zones. In the first, circumscribed by

16) $$r_3(\ell) = (\ell-\ell_1)\tan\alpha = -r_1(\ell)$$

the effective solid angle of collection is constant at (small angle approximation)

17) $$\Omega(o,\ell) = \frac{\pi}{4}\,\frac{d^2}{\ell^2}$$

while in the outer one, circumscribed by $r_2(\ell)$, we have

18) $$\Omega(r,\ell) = \frac{\pi}{4}\,\frac{d^2}{\ell^2}\,\frac{r_2(\ell)-r(\ell)}{r_2(\ell)-r_1(\ell)} = \frac{\pi}{4}\,\frac{d}{\ell^2}\Big[r_2(\ell)-r(\ell)\Big]$$

giving for the efficiency in this range of ℓ, normalized to $\nu = o, \ell = o$ and an Ω_1 observation solid angle

19)

$$E(\ell) = \frac{3}{\pi\, r_2^2(\ell)} \left\{ \int_o^{-r_1(\ell)} 2\pi r(\ell)\, \frac{\pi d^2}{4\ell^2}\, \frac{1}{2\pi(1-\cos\alpha)} \left[1 - \frac{r(\ell)}{r_2(\ell)}\right] \partial r(\ell) + \right.$$

$$\left. \int_{-r_1(\ell)}^{r_2(\ell)} 2\pi r(\ell)\, \frac{\pi d}{4\ell^2}\, \frac{r_2(\ell) - r(\ell)}{2\pi(1-\cos\alpha)} \left[1 - \frac{r(\ell)}{r_2(\ell)}\right] \partial r(\ell) \right\} =$$

$$= \frac{3}{4} \frac{d}{\ell^2 r_2^3(\ell)(1-\cos\alpha)} \left\{ d \int_o^{-r_1(\ell)} \left[r_2(\ell)\, r(\ell) - r^2(\ell) \right] \partial r(\ell) + \int_{-r_1(\ell)}^{r_2(\ell)} \left[r^3(\ell) - 2r^2(\ell)\, r_2(\ell) + r(\ell) r_2^2(\ell) \right] \partial r(\ell) \right\}$$

$$= \frac{3}{4} \frac{d}{\ell^2 r_2^3(\ell)(1-\cos\alpha)} \left\{ d \left[\frac{1}{2}\, r_2(\ell) r^2(\ell) - \frac{1}{3} r^3(\ell) \right]_o^{-r_1(\ell)} + \left[\frac{1}{4}\, r^4(\ell) - \frac{2}{3} r^3(\ell)\, r_2(\ell) + \frac{1}{2} r^2(\ell) r_2^2(\ell) \right]_{-r_1(\ell)}^{r_2(\ell)} \right\}$$

$$= \frac{3}{4} \frac{d}{\ell^2 r_2^3(\ell)(1-\cos\alpha)} \left\{ d \left[\frac{1}{2}\, r_2(\ell) r_1^2(\ell) + \frac{1}{3} r^3(\ell) \right] + \left[\frac{1}{2}\, r_2^4(\ell) - \frac{1}{4} r_1^4(\ell) + \frac{2}{3} r^3(\ell)\, r_2(\ell) - \frac{1}{2} r_1^2(\ell) r_2^2(\ell) \right] \right\}$$

which can be simplified to

$$20)\quad E(\ell) = \frac{d^2}{64\ell^2(1-\cos\alpha)}\left[d^3 - 2d^2\ell\tan\alpha + 12d\ell^2\tan^2\alpha + 8\ell^3\tan^3\alpha\right]\frac{1}{\left(\frac{d}{2} + \ell\tan\alpha\right)^3}$$

and further

$$21)\quad E(x) = \frac{\tan^2\alpha}{2(1-\cos\alpha)}\quad\frac{x^3+3x^2-x+1}{x^2(1+x)^3}$$

from which the effective pathlength from ℓ_1 to infinity can be calculated

$$22)\qquad t_{>\ell_1} = \ell_1\,\frac{\tan^2\alpha}{2(1-\cos\alpha)}\int_1^{\infty}\frac{x^3+3x^2-x+1}{x^2(1+x)^3}\,\partial x =$$

which can be solved from tables to give

$$23)\qquad t_{\ell_1} = \left(\frac{7}{2} - 4\ln 2\right)\frac{\tan^2\alpha}{2(1-\cos\alpha)}\,\ell_1 \approx \left(\frac{7}{2} - 4\ln 2\right)\ell_1 = 0.727\ell_1$$

in the small angle approximation, and so we have for the effective pathlength of the system

$$24)\qquad t = (7 - 8\ln 2)\ell_1 = 1.45\ell_1 = \frac{0.727d}{\tan\alpha}$$

Here we have for E(X) the following values, which reflect the extent to which different depths (in terms of diameter) contribute to the signal.

x	0	½	1	3/2	2	5	10
E(x)	1	0.704	0.500	0.274	0.176	0.0363	0.0097